Volume 2
Texas A&M University
Oceanographic Studies

Contributions on the Physical Oceanography of the Gulf of Mexico

L. R. A. Capurro

Editorial Director
Department of Oceanography, UNESCO
Paris, France
Lecturer, Texas A&M University, College Station, Texas

Joseph L. Reid

Research Oceanographer, Department of Oceanography
Scripps Institution of Oceanography, La Jolla, California

1 Winter Circulation Patterns and Property Distributions

Worth D. Nowlin, Jr.

Abstract

Based on their characteristic properties, the water masses of the Gulf of Mexico and their vertical stratification are discussed. The *T-S* relationships specific to the region are presented. For the basin waters, below a sill depth of about 2000 m, the potential temperature, salinity and dissolved-oxygen concentrations show no measurable horizontal variation, although weak vertical density gradients evidence slight positive stability. Variations in the characteristics of the water in the following layers are shown, and the likely origins of these water masses are identified: North Atlantic Deep Water, Subantarctic Intermediate Water, oxygen minimum layer and Subtropical Underwater. For the winter season, the property distributions in the mixed surface layers are described.

On the basis of dynamic computations and GEK measurements, the general winter circulation patterns within the Gulf are examined. The mode most often observed in the eastern Gulf is one dominated by the Loop Current; water enters through Yucatan Strait as the Yucatan Current and flows in a clockwise loop which extends well into the Gulf and exits via Florida Strait. The extent of penetration and location of this loop is quite variable. In other seasons, large current rings are known to separate from the Loop Current. In contrast, the winter circulation in the western Gulf seems more predictable; it consists primarily of a clockwise cell centered over the western central Gulf, having broad westward flow for its southern limb, a narrow east northeastward flow for its northern limb and flanked to the north by a west-southwestward current along the outer Texas-Louisiana shelf.

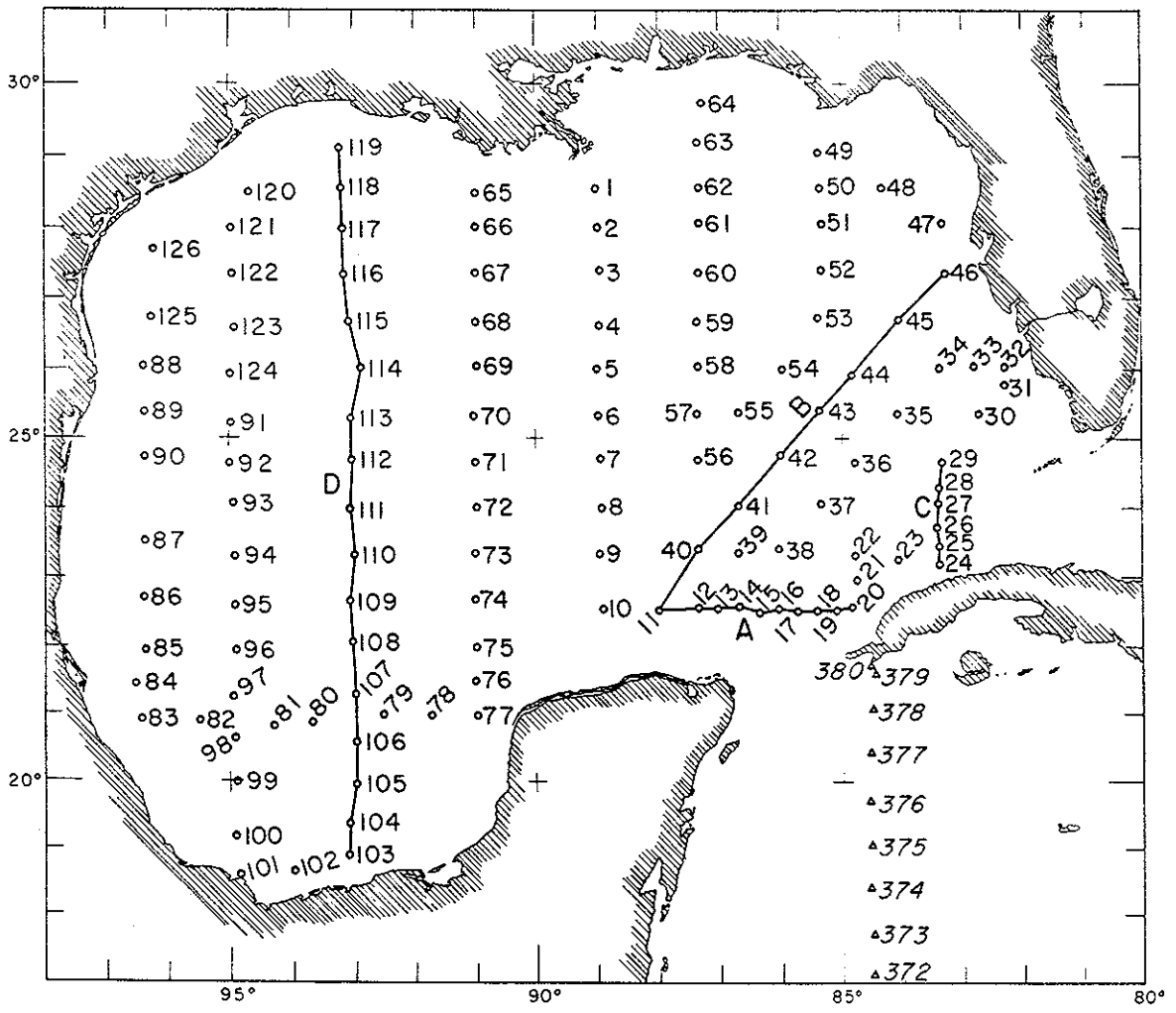

Figure 1-1. Stations occupied during Hidalgo *62-H-3, February-March, 1962 (circles), and* Crawford *Cruise 17, February-March, 1958 (triangles). Lines indicate vertical sections discussed in text.*

Introduction

This paper presents a characterization of the Gulf of Mexico waters for the winter season. There have been three major exploratory cruises within the Gulf during winter. During 25 January through 27 April 1932, the *Mabel Taylor*, under the direction of A.E. Parr from Yale, occupied 69 hydrographic stations in the Gulf of Mexico; Parr presented the results in 1935. Unfortunately, there is understandable uncertainty attached to the reported depths for these *Mabel Taylor* samples because Parr did not have unprotected reversing thermometers aboard during the cruise. The *Atlantis* produced reliable hydrographic data from 98 Gulf stations occupied between 15 February and 13 April of 1935. Neither of these cruises occupied a sampling pattern adequately uniform or dense to

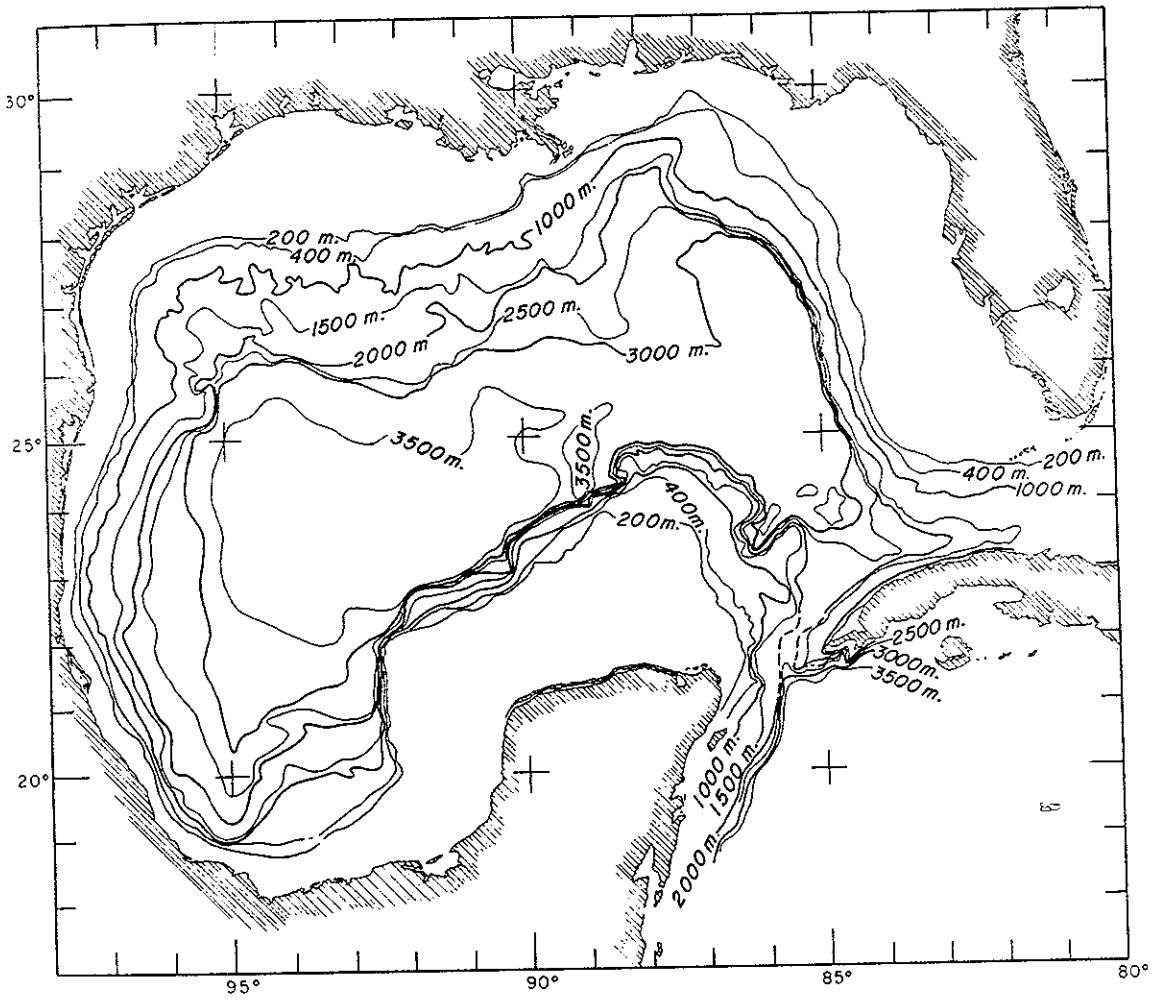

Figure 1-2. Bathymetry of Gulf of Mexico based on U.S. Coast and Geodetic Survey Chart 1007 and soundings on file at Department of Oceanography, Texas A&M University.

describe the entire Gulf. In 1962, the *Hidalgo* of Texas A&M University was used by H. J. McLellan and W.D. Nowlin, Jr. in a hydrographic survey to obtain data that might for the first time fully characterize the Gulf of Mexico waters during the winter. This cruise (62-H-3), which was executed as rapidly as the vessel's capability permitted—from 12 February through 31 March—systematically covered the entire Gulf of Mexico. Figure 1-1 shows the station positions, numbered serially in the sequence of their occupation. The maximum sampling depth at most stations was near the bottom; Figure 1-2 shows the general bathymetry of the Gulf.

Although data from many cruises are utilized, the cornerstone for this description is the winter characterization of the Gulf of Mexico based on the findings from Cruise 62-H-3. Unless otherwise

stated, the data presented and inferences therefrom are from Cruise 62-H-3 and are meant to represent conditions during only February and March of 1962. This point is emphasized because of the temporal variability in the strength and distribution of circulation features in the Gulf shown by other studies, e.g., the work of Cochrane (1963, 1965) dealing with the Yucatan Current in and near Yucatan Strait. Because of this temporal variability, circulation patterns arrived at by combining data collected over a period of many years and seasons (such as the very complicated averaged dynamic topographies presented by Duxbury in 1962) may not represent conditions typical of the region during any season.

When planning Cruise 62-H-3 a careful evaluation of existing data, including those collected in other seasons of the year, and interpretations of data were made. The sequence of observations that ranks second to the 1962 survey in approaching a synoptic survey of the entire Gulf of Mexico is the series of 124 hydrographic stations occupied between 22 April and 21 August 1951 by the *Alaska* of the U. S. Fish and Wildlife Bureau in cooperation with Texas A&M University. Combining data from these three cruises, Austin (1955) presented a pattern for the dynamic topography of the sea surface relative to the 1000-db surface (Figure 1-3); Collier et al. (1958) presented a similar pattern for the 500-db dynamic topography relative to 1000 db. These geopotential anomalies may be interpreted as indicating a very complicated circulation pattern within the central and western Gulf. The circulation within the eastern Gulf, except over continental shelves, seems dominated by the Loop Current, which is the Yucatan Current's downstream continuation through the Gulf and into the straits of Florida.

Every "high" and "low" of the Gulf circulation as inferred by Austin (Figure 1-3) was intersected by at least one line of stations on the 62-H-3 cruise plan. In regions where existing data indicated large horizontal current shear, an effort was made to space stations rather closely on transects perpendicular to the indicated current directions. Nansen bottles and paired reversing thermometers were used at each hydrographic station to collect water samples and to measure the *in situ* temperatures and depths of the samples. The water samples were analyzed aboard ship by using a conductivity-type salinometer (University of Washington, No. 12) for salinity and the Winkler method for dissolved oxygen. Because of the apparently limited accuracy of the dissolved oxygen measurements, data from other cruises have been used to establish the oxygen distribution within the deep waters of the Gulf. The observed hydrographic data as well as meteorological observations are available from the National Oceanographic Data Center or in an unpublished data report (Ref. 62-16D, Department of Oceanography and Meteorology, The A.&M. College of Texas). Bathythermograms and geomagnetic electrokinetograph (GEK) current measurements were made at one-hour intervals while underway between stations.

Characteristic *T-S* Relationship

Figure 1-4 shows temperature versus salinity for all observations at temperatures lower than 17°C and for the near-surface layers at each of 17 stations in the regions of inflow and outflow. For the realm below 17°C (representing 849 data points) the plot shows a remarkable uniformity, indicating that the waters constitute essentially a single system. Comparison with historical data indicates no departures from this characteristic curve that could not be attributed to observational error.

If the data are examined on a regional basis the interagreement between stations is even more remarkable. Based on the 62-H-3 data, Caruthers (1969) made a careful comparative analysis of the potential temperature (θ) versus salinity (S) relation for the intermediate depth waters. Potential temperatures were obtained using the tables of Helland-Hansen (1930). The analysis was restricted to depths between 100 m and 1200 m and to potential temperatures between 4° and 20°C. A "standard" θ–S relation was selected, and regional deviations from this standard were quantified and discussed.

Stations 16-22 and 38, within the water of the

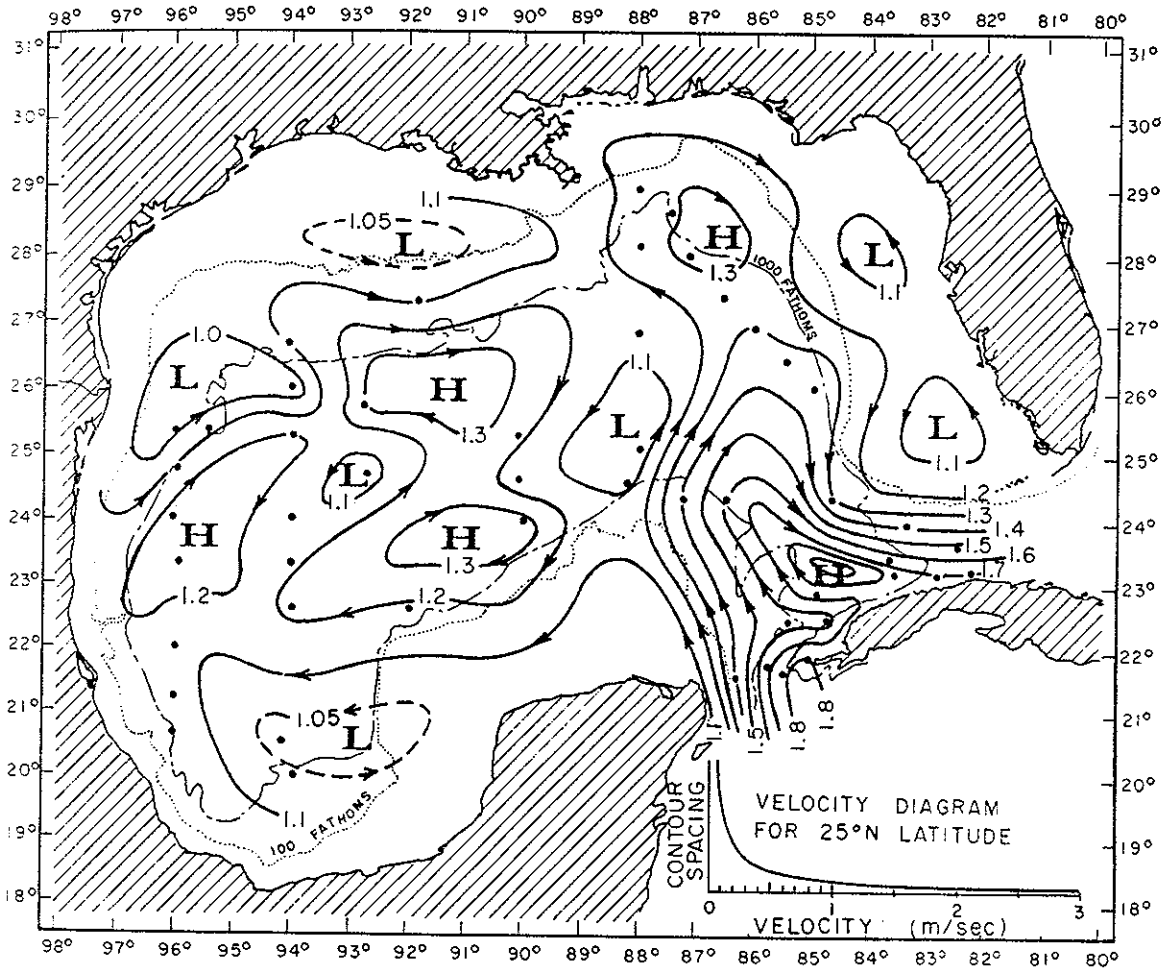

Figure 1-3. Dynamic topography of surface relative to 1000-db surface; Alaska *Cruises 1-1A, 2-1B and 3-1C, 22 April-21 August, 1951. (After Austin, 1955: Figure 2.)*

eastern Gulf bounded by the Loop Current and Cuba, were used to define the standard relation. Caruthers found that according to the F-test the best fit to these 33 temperature-salinity pairs is a seventh degree polynomial in potential temperature representing salinity by

$$S = \sum_{n=0}^{7} A_n (\theta/10)^n.$$

The standard error is 0.0045 per mil if the coefficient $A_0, \ldots, A_7$ have the values: 32.58314, 23.11518, −82.50041, 143.1953, −135.2648, 71.99103, −20.27993, 2.34921

For the 62-H-3 data Caruthers computed the differences between the observed salinity and the salinity computed from the standard relation for the corresponding temperature. For each station, polynomials were fitted to these differences. It was noted that "the water type found at 14°C is very constant and represents the zero crossing" of these graphs. Caruthers (1969) also confirmed in

quantitative form the observations that there is a tendency for the salinities near the minimum, which occurs at temperatures below 14°C, to uniformly increase and a tendency for salinities at temperatures above 14°C to decrease as one moves into the northern or western Gulf.

Figure 1-4. Temperature versus salinity, Hidalgo *62-H-3, for all observations with temperatures less than 17°C and for the near-surface waters at 17 stations in the regions of inflow and outflow. For temperatures greater than 17°C,* T-S *relations are ploted for 10* Crawford *stations occupied in the Caribbean. See Figure 1-1 for station locations.*

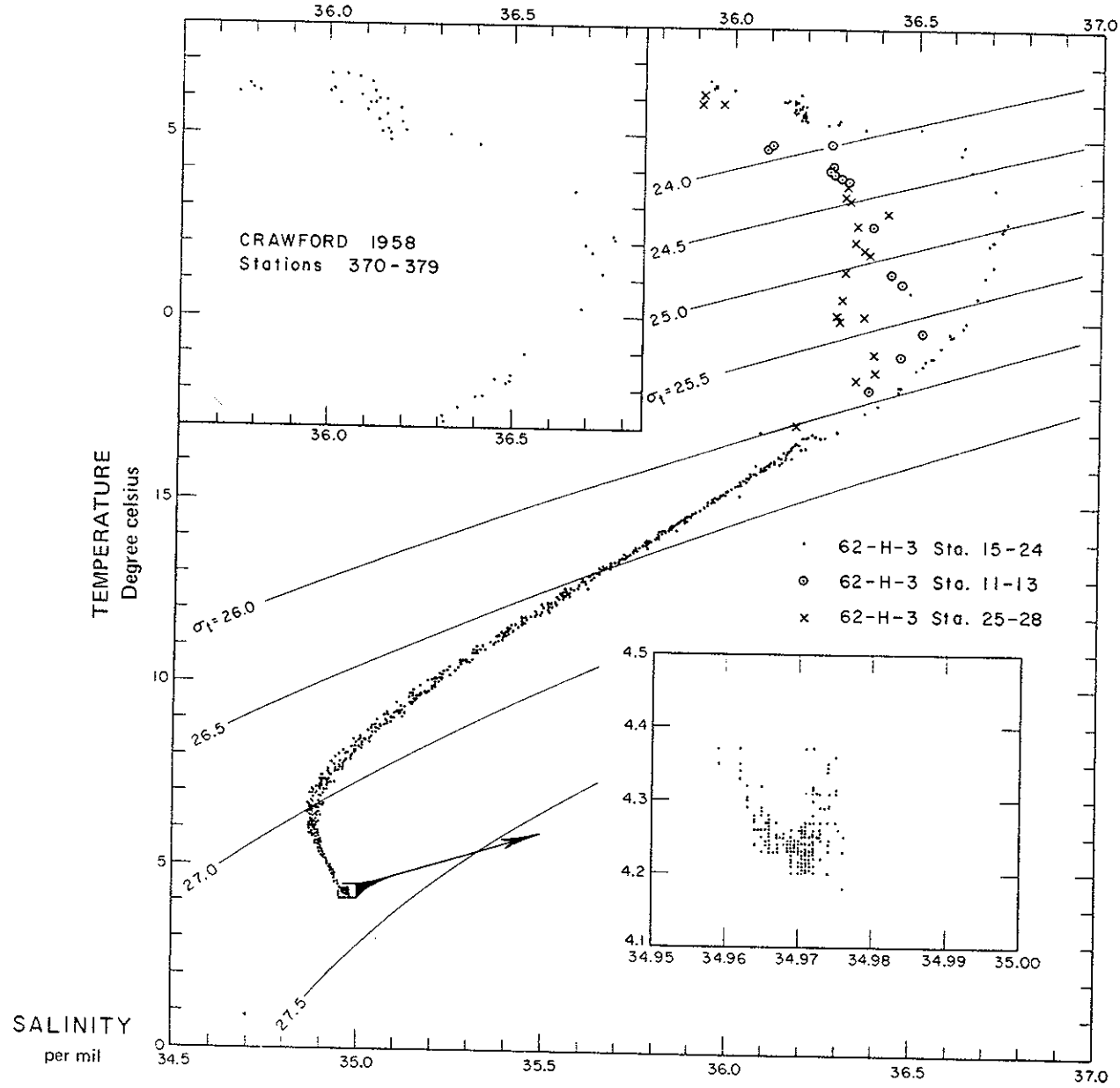

The salinity minima, which occur in the eastern Gulf at temperatures of approximately 6.3°C, are specific to the remnant of Subantarctic Intermediate Water. For comparison, within the Antillean sector of the North American Basin of the North Atlantic, the core of this Subantarctic Water layer (Wüst, 1964) is found at depths of 700-850 m, with salinities as low as 34.60 per mil and corresponding temperatures as low as 5.2°-5.6°C. On entering the eastern Caribbean this core layer has typical minimum salinities (Wüst, 1964: plate XVI) just under 34.70 per mil, with temperatures around 5.7°C. There is a consistent spatial increase in salinity and temperature within this core layer as one progresses eastward through the Caribbean Sea.

Within the western Gulf of Mexico this feature appears to be eroded to an extent that increases the minimum salinity some 0.02-0.03 per mil and decreases the associated temperature at the minimum some 0.1-0.2°C relative to the characteristics as this water enters the eastern Gulf. The width of the characteristic plot (Figure 1-4) from 5-14°C is occasioned by this mixing activity. For the waters in this potential temperature range, the maximum departure of salinity from the standard θ–S relation was obtained at each station from Caruthers' (1969) fitted polynomials. These values were plotted, and the contoured number field is presented as Figure 1-5. (Remember that the standard relation is based on data from stations within the Loop Current regime.) Salinity increases seem to become regularly greater with increasing distance into the Gulf; the maximum anomaly values of 0.04 per mil occur in the Bay of Campeche, which is separated from the Yucatan Strait inflow by the broad shelf of the Yucatan Peninsula, a barrier to waters at intermediate depths. Caruthers (1969) notes that the maximum increase of salinity occurs around 9°C instead of at the salinity minimum.

In Figure 1-4 the characteristics of water below 4.4°C are shown in an insert. The pressure effect leads to an increase in *in situ* temperature with depth below 2000 m, although potential temperature appears to decrease slowly to at least 3000 m, as discussed below. Similarly, the salinity of the deep water is shown to increase slightly, though continuously, with depth.

The relationship between potential temperature and salinity for observations from depths greater than 1400 m is shown in Figure 1-6. Comparison of this θ–S plot for waters of the Gulf Basin with a corresponding plot for waters of the Yucatan Basin (*Crawford* Sts. 372-379; Figure 1-1) will convince one that at any given potential temperature in the range 4.01-4.15°C, significant differences in salinity between the waters of the two basins do not exist, i.e., the salinity differences do not exceed 0.006 per mil, which is roughly twice the error claimed for the conductive measurement of salinity.

The T-S curve from 4.5-17°C is similar in form to that found in the Caribbean (Wüst, 1964, Figure 3); but there especially in the east, the salinity minimum is a much more distinct feature. This is consistent with the west-northwestward flow of water through the Caribbean and into the Gulf through Yucatan Strait.

All stations off the shelf display a salinity maximum within the upper 200 m. For Sts. 15 through 24 this feature traces a smooth curve, with a maximum near 22.5°C and 36.75 per mil—rather like Wüst's (1964: Figure 3) case of Subtropical Underwater for the Caribbean. This same relationship shows clearly (insert, Figure 1-4) at *Crawford* Sts. 370 to 379 taken across the western Yucatan Basin in February and March 1958. Within the Gulf, those waters having such a T-S relationship (i.e., that shown for Sts. 15 to 24) are commonly bounded by the Loop Current, comprised of the Yucatan Current and its downstream extension through the eastern Gulf into the Florida Straits. Wennekens (1959) gave the name Yucatan Water to that having this set of characteristics. A specific name does not seem apropos, since these characteristics are just the same as for the upper waters of the northwest Caribbean. In addition to these waters bounded by the Loop Current, anticyclonic current rings surrounding

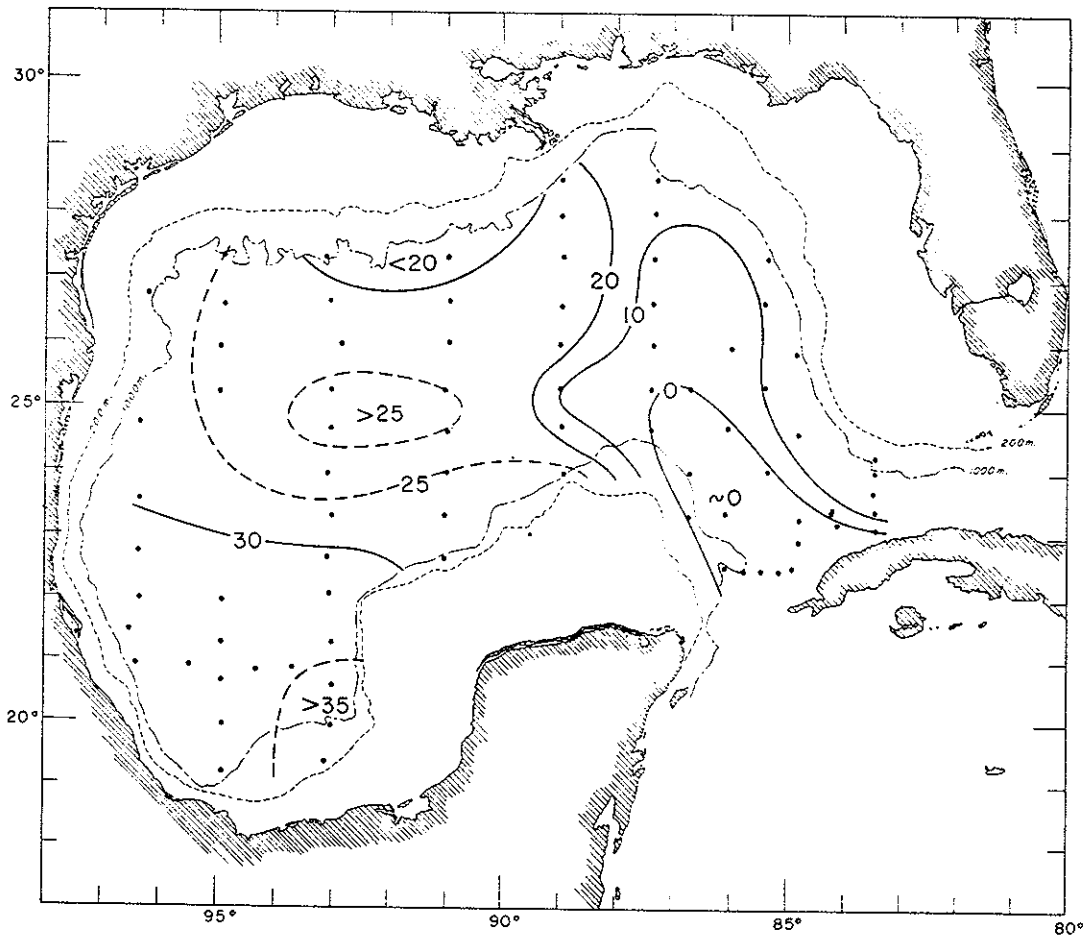

Figure 1-5. For waters with potential temperatures between 5° and 14°C, the maximum departure of salinity parts per million from "standard" potential temperature-salinity relation for Gulf given by Caruthers (1969). Positive values indicate observed salinity at individual station was greater than standard salinity at same potential temperature. Analysis based on Hidalgo *62-H-3 data from the station positions indicated.*

waters of these same characteristics are known (Nowlin et al., 1968) to become detached from this Loop Current in the eastern Gulf. (See Chapter 6 for a detailed description.)

Wennekens (1959) has indicated that the Yucatan Water, at least at times, is found in Florida Straits as far downstream as the Miami-Bimini region. Wenneken's data indicate that the northern limit of this water in the southern Florida Straits is usually about midway between Cuba and the western Florida Keys. On Cruise 62-H-3 definite evidence of this water was found in Section *C* at St. 24 only. Its distribution within the Gulf is discussed further below.

Sts. 11 through 13 in the western part of Yucatan Section *A* and Sts. 25 through 28 in the Florida Straits Section *C* show less regular *T-S* curves and display salinity maxima at lower salinities and temperatures. This feature was noted by Cochrane (1963) for the Yucatan Strait, and his

suggestion (Cochrane, 1965) that part of the Yucatan Current flows inside Cozumel Island and Arrowsmith Bank invites speculation that vigorous vertical mixing may occur in this part of the passage.

Based on *Hidalgo* 62-H-3 data, Wilson (1967) estimated quantitatively the volumes of water in the Gulf of Mexico of different classes according to potential temperature-salinity characteristics. Much of the Gulf water was shown to be derived from the Caribbean water by mixing. Wilson concludes that "a dominant factor in the creation of new water types in the Gulf of Mexico appears to be the reduction in strength of the salinity maximum associated with the Subtropical Underwater," and that "the region of the Campeche Bank appears to be a focal point for water mass formation, modification and distribution in the Gulf of Mexico." According to Wilson's volumetric distributions by potential temperature-salinity classes, the occurrence of water in classes which differ from water found also in the Caribbean is expect-

Figure 1-6. Potential temperature-salinity relationships for all observations from deeper than 1400 m on Hidalgo *62-H-3, Gulf of Mexico.*

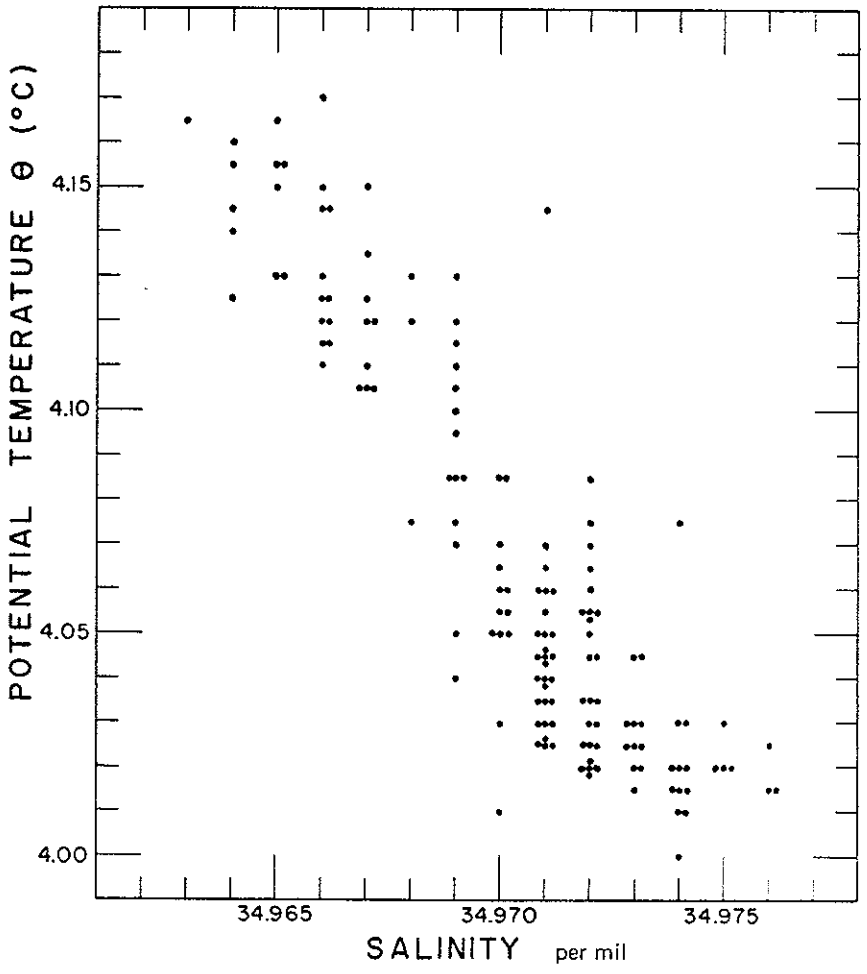

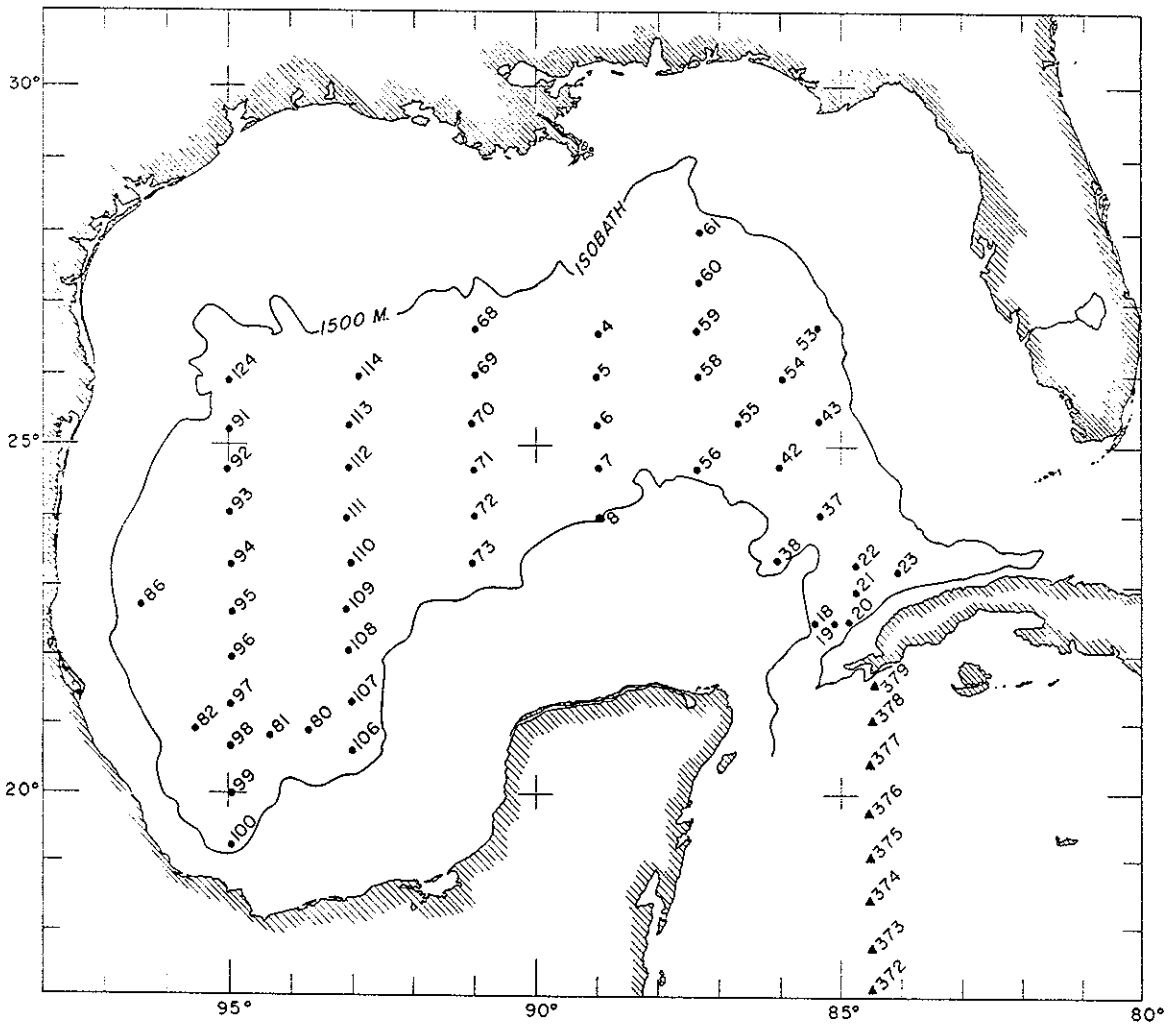

Figure 1-7. Location of stations occupied during Hidalgo *62-H-3 (solid dots) where observations at depths greater than 1500 m were made. Location of* Crawford *Cruise 17, Sts. 372-379 (solid triangles), in the western Caribbean are also shown.*

edly more common in the western than in the eastern Gulf. These conclusions support the previously mentioned suggestions regarding vertical mixing.

Water Masses and Stratification

The Basin Waters

The central Gulf of Mexico, having depths in excess of 3400 m, is a basin isolated from the adjacent Caribbean Sea by a sill with a controlling depth of roughly 2000 m (Figure 1-2); the sill depth in the Yucatan Channel has not been determined with precision. Figure 1-7 shows the 52 stations at which observations from depths greater than 1500 m were obtained. The characteristics and origins of the waters below 1500 m are discussed in this section.

Salinity and Potential Temperature. Figure 1-8 shows a composite plot of salinity versus depth for

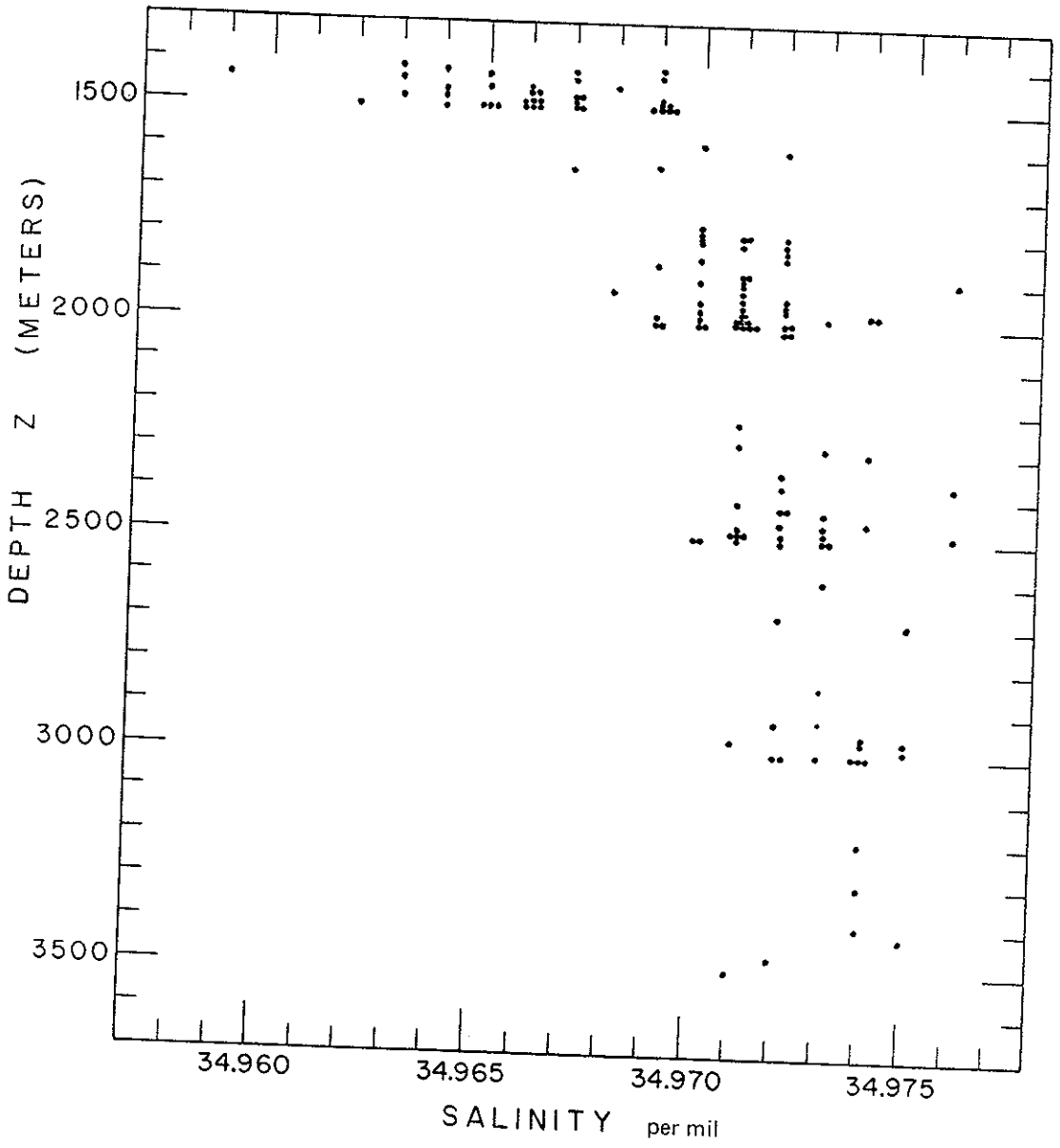

Figure 1-8. Salinity-depth relationships for all observations from deeper than 1400 m on Hidalgo *62-H-3, Gulf of Mexico.*

all observed depths below 1400 m at the 52 deep stations of Figure 1-7. From 2000 m to the maximum depth sampled, the range in observed salinity was only 0.008 per mil. All salinity observations from depths greater than 1500 m were fitted to both first-and second-degree polynomials (in depth) by the method of least squares. The resulting linear and quadratic forms, each with a standard error of 0.0015 per mil, appeared to be equally good. Salinity values and gradients at standard depths were obtained from this linear fit and are presented in Table 1-1. This trend line (omitted

Table 1-1
The Mean Stability Parameter, E,
from Mean Values and Gradients of T and S at Stated Depths

Z (m)	T (°C)	S (per mil)	$dT/dZ \times 10^3$ (°C m^{-1})	$dS/dZ \times 10^3$ (per mil m^{-1})	$E \times 10^8$ (m^{-1})
2000	4.23	34.971	0.034	0.002	1.3
2500	4.26	34.972	0.077	0.002	0.8
3000	4.31	34.973	0.120	0.002	0.2

from Figure 1-8 for clarity) indicates that throughout this deep water salinity continued to increase with depth, with a gradient of some 0.002 per mil per 1000 m. Although the error claimed in the measurement of salinity by the conductive method is ± 0.003 per mil or more, this gradient appears to be real rather than due to scatter. Even if this gradient is real, however, it may be a measurement of something other than salinity as usually defined, e.g., a slight departure from constancy of composition.

In Figure 1-9 it is seen that a general decrease in potential temperature with depth was observed from 1400 to 3000 m; these potential temperatures were computed from tables given by Helland-Hansen (1930). The potential temperatures for all observed depths greater than 1500 m were fitted to several alternate functional forms. The form chosen was the second-degree polynomial in depth,

$$\theta = 4.334 - 2.139 \times 10^{-4} Z + 3.596 \times 10^{-8} Z^2, \quad (1.1)$$

with θ in degrees Celsius and Z in meters; this gave a standard error of 0.012 C degrees. Resulting mean potential temperatures for selected depths are presented in Table 1-2; these values agree to three significant figures with the arithmetic means of the potential temperatures observed within a depth range of 50 m on either side of the tabulated depths. Although the number of observations below 3000 m is small, it may be said that the potential temperature does not decrease further below this depth.

That the vertical gradients of both potential temperature and salinity were observed to be small below the 2000-m depth is consistent with the concept of a basin isolated by a sill whose controlling depth is 2000 m or less. The observed vertical gradients indicate diffusion of salt (upward) and heat (downward at least to 3000 m). No significant pattern of horizontal variations in salinity or potential temperature was discernible below 2000 m.

Table 1-2
Mean Potential Temperatures (θ)

Depth (m)	θ(°C)
2000	4.050
2500	4.024
3000	4.016
3500	4.026

Stability of the Basin Waters. On the basis of the vertical distribution of potential temperature, the waters of the basin appear to be stable down to 3000 m. Moreover, if the salinity gradient is to be accepted, this stability is enhanced, and it may be that the waters are stable to the bottom.

Since the ranges of both potential temperature and salinity in Figures 1-8 and 1-9 are limited, it is easily possible to overestimate the degree of positive stability from a consideration of these figures. It seems worthwhile, therefore, to consider some parameter whereby the vertical stability of these waters may be quantitatively compared with that of waters in other areas. Such a quantitative

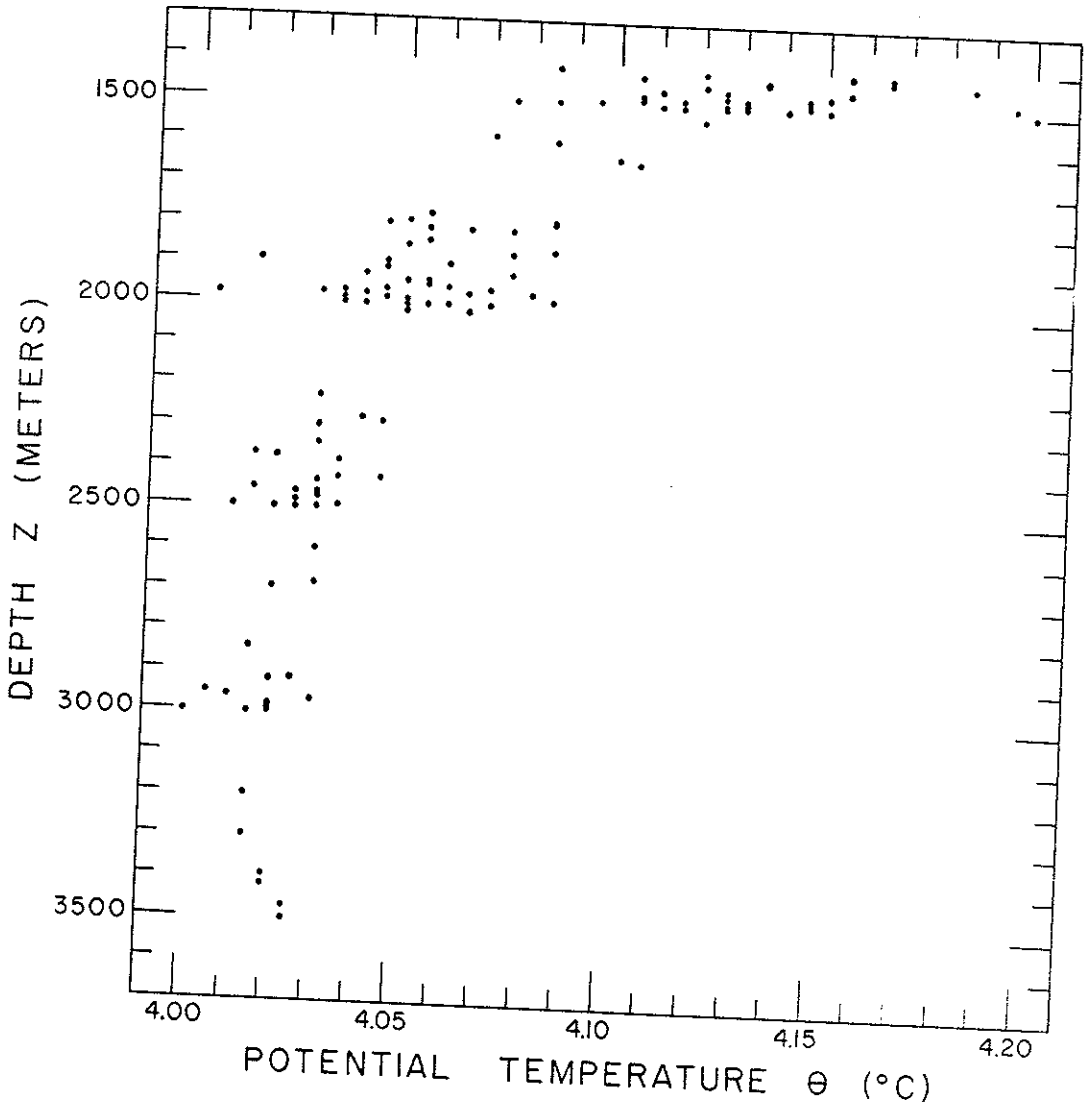

Figure 1-9. Potential temperature-depth relationships for all observations from deeper than 1400 m on Hidalgo *62-H-3, Gulf of Mexico.*

measure is provided by the Hesselberg-Sverdrup (1915) stability parameter, E, an equivalent of which may be defined by

$$E = (1/\rho)[(\partial\rho/\partial S)(dS/dZ) + (\partial\rho/\partial T)(dT/dZ - \gamma)],$$

where: ρ is density, S salinity, T temperature, and Z depth (increasing downward); DS/dZ and dT/dZ denote environmental gradients; $\partial\rho/\partial S$ and $\partial\rho/\partial T$ denote thermodynamic partial derivatives; γ denotes the increase in temperature per unit increase in depth under adiabatic conditions.

The mean values of E and the mean values and mean gradients of salinity and temperature (denoted by superior bars) from which they were computed are presented in Table 1-1. The values and gradients of temperature were obtained from a

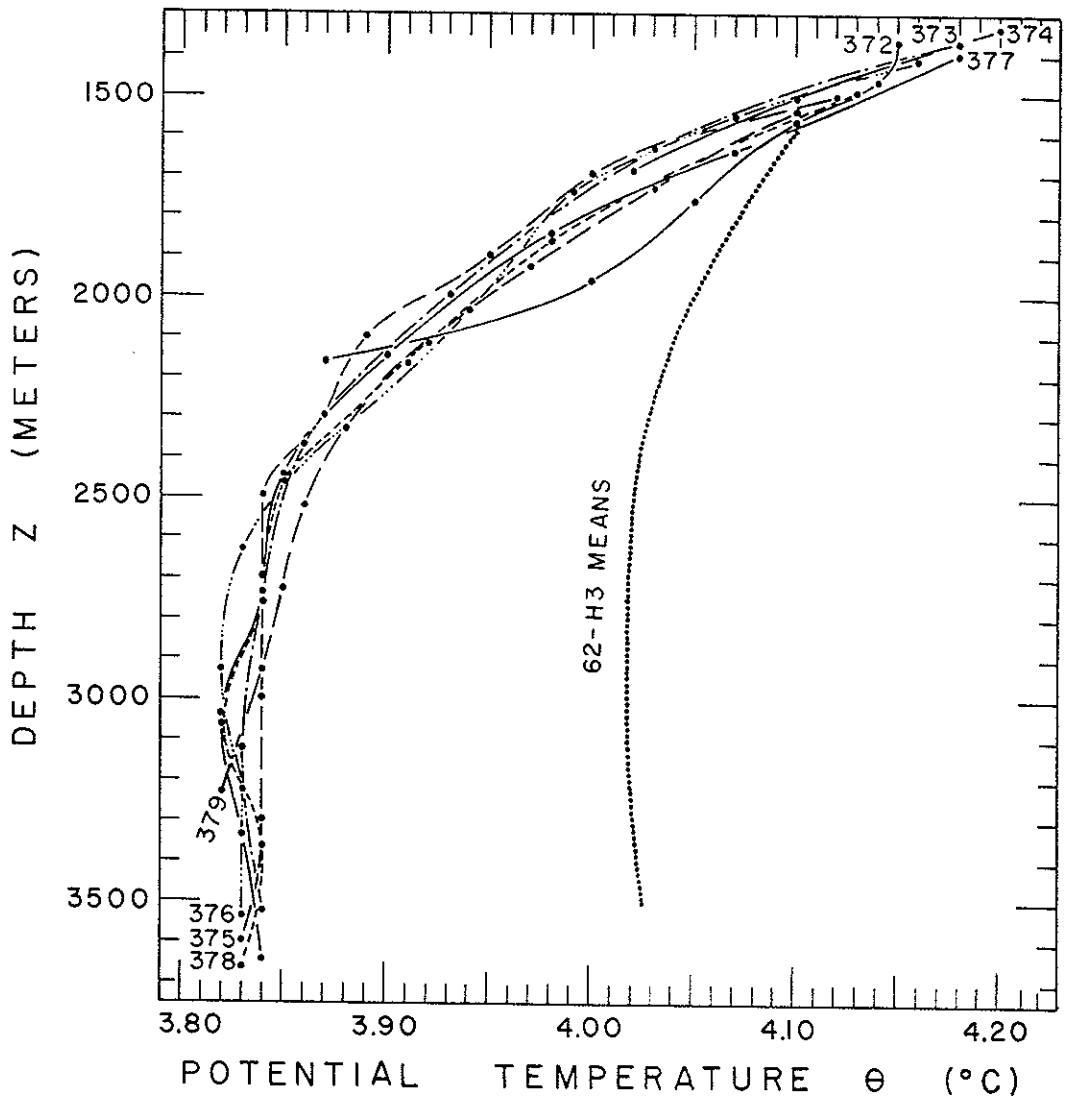

Figure 1-10. Potential temperature-depth relationships for Crawford *Cruise 17, Sts. 372-379. Range of* Hidalgo *62-H-3 observations shown.*

regression analysis of temperature data collected on Cruise 62-H-3 from depths greater than 1500 m. The standard error of the resulting curve fit was 0.014°C. The values of thermodynamic partial derivatives were taken from Hesselberg and Sverdrup (1915).

Although it seems significant that positive stability is indicated as the mean condition, the values of E are so small as to strain the accuracy of the data from which they were computed. If these values of the stability parameter are compared with values available for comparable depths in open ocean areas, where $E \times 10^8$ is of the order of 10 m^{-1}, it is concluded that the Gulf of Mexico Basin waters have nearly neutral stability, as expected. Stability computations based on data from

consecutive sampling depths at individual stations also indicate stable conditions with few exceptions: 11 stations evidenced neutral conditions; St. 110 indicated unstable conditions, $E \times 10^8 = -1.8 m^{-1}$, in the depth range 2750-3250 m.

Origin of the Basin Waters. The lack of any discernible tendency toward horizontal variations in salinity or potential temperature within the basin has been mentioned. This seems to indicate that either the basin waters had a common source or their residence time is of a magnitude sufficient to insure that horizontal gradients have been destroyed by exchange processes. Since the only major inflow to the Gulf at present is through the Yucatan Channel, it is reasonable to compare the characteristics of the waters of this basin with those of the Cayman Basin.

Figure 1-10 shows θ-Z curves for Sts. 372-379 of *Crawford* Cruise 17, located on a north-south line between the western tip of Cuba and Honduras (Figure 1-1). Also pictured (Figure 1-10) is the graph of the least-squares fit, equation (1-1), relating potential temperature and depth as observed on Cruise 62-H-3. If it is assumed that waters from the Cayman Basin are presently displacing the bottom waters of the Gulf of Mexico Basin, then consideration of potential temperatures leads to an estimated maximum controlling sill depth of between 1650-1900 m (less than 1800 m if *Crawford* St. 372 is ignored). If it is assumed that the bottom waters of the Gulf Basin have a greater potential density than the present Yucatan waters at the controlling sill depth, then Yucatan waters may presently be flooding the Gulf Basin at some depth between 1500 m and the bottom. In this case the controlling sill depth must be less than 1900 m. It is seen, however, that this sill depth must be at least 1400-1500 m, for at these depths the θ-Z curves for the Yucatan and Gulf waters coincide. Moreover, if the controlling sill depth is within this shallower range, the interpretation might be that the Gulf Basin was filled at some past time (when the distribution of temperature within the Yucatan Basin differed from that evidenced by the *Crawford* data).

During June, 1967, a number of deep hydrographic stations were made in the Gulf of Mexico aboard *Alaminos* on Cruise 67-A-4. Two deep stations were also made in the Yucatan Basin. (For station locations, see Figure 1-11.) Although the values of adiabatic cooling that were applied to *in situ* temperatures to determine potential temperatures were based on data presented by Cox and Smith (1959) rather than on the Helland-Hansen (1930) data, the results (Nowlin et al., 1969: figure 2) substantiate Figure 1-10. Curves of potential temperature versus salinity drawn from 67-A-4 data taken on opposing sides of the Yucatan sill intersect at about 1550 m.

It must be emphasized that the controlling sill depth as discussed is only an estimate. The difficulty of accurately relating the controlling sill depth to the available hydrographic data is reflected in the following statements:

1. Unless isothermal surfaces are horizontal within the Yucatan Basin in the 1400-2000-m depth range, the water found some hundreds of kilometers removed from the sill cannot be expected to represent the water available for inflow into the Gulf of Mexico at the same depth.
2. Since the northward currents through the Yucatan Channel are thought to extend practically to the bottom and affect the slope of isosteric surfaces, it is possible that the intensity of this flow (not necessarily stationary) may determine the greatest depth from which Caribbean waters enter the Gulf.
3. Even though no horizontal gradients of conservative properties have been observed within the Gulf Basin, such gradients may exist near the bottom in the area north of the Yucatan sill if Caribbean waters are presently moving northward in a downslope flow and displacing the bottom waters of the Gulf Basin.

In a foregoing section, Yucatan and Gulf Basin waters were compared on the basis of

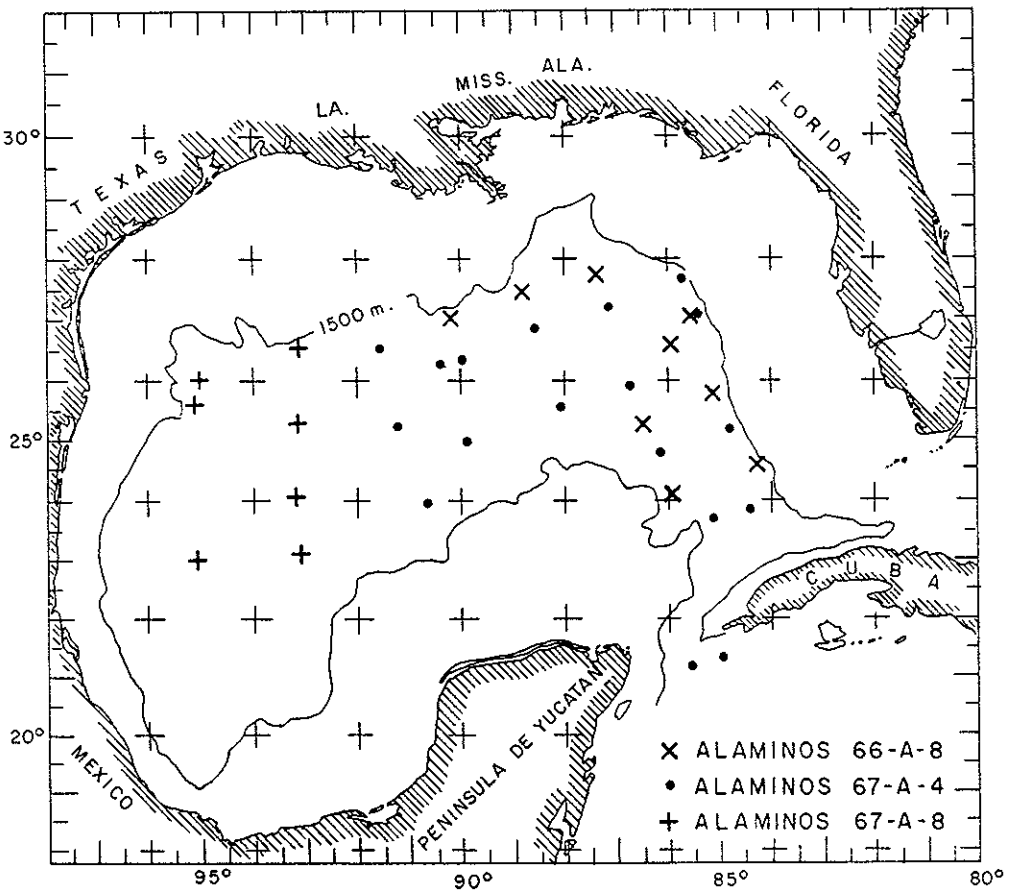

Figure 1-11. Locations of stations on Alaminos *Cruises 66-A-8 (1-24 June 1966), 67-A-4 (10 June-1 July 1967) and 67-A-8 (9-12 September 1967) from which data were utilized.*

salinity. The relationships of potential temperature versus salinity near sill depth in the two basins are quite similar and so are consistent with the idea of present-day displacement of Gulf bottom water by Cayman water.

Distribution of Dissolved Oxygen

In this section, oxygen data obtained in 1966 and 1967 are compared with selected data obtained in 1935, 1958, 1959, 1962 and 1964. It is shown that there is no clearly discernible horizontal variation in dissolved oxygen in the basin waters of the Gulf of Mexico.

The available dissolved oxygen measurements provide areal coverage of the entire Gulf Basin and were obtained on cruises of the *Atlantis*, the *Hidalgo* and the *Alaminos*. The *Atlantis* in 1935 and the *Hidalgo* in 1958 (58-H-4) provided observations principally from the central eastern Gulf; observations were obtained from the western part on the *Hidalgo* in 1958 and 1959 (58-H-1, 59-H-2) and on the *Alaminos* in 1964 (64-A-2, 64-A-3); observations from the entire Gulf Basin were obtained on the *Hidalgo* in 1962 (62-H-3) and on the *Alaminos* in 1966 and 1967 (66-A-8, 67-A-4, 67-A-8); and observations in the Yucatan Basin were obtained on the *Alaminos* in 1967

(67-A-4). The *Atlantis* data are available from the Woods Hole Oceanographic Institution, the other data from the Department of Oceanography at Texas A&M University. Figure 1-11 shows the locations of the 1966 and 1967 *Alaminos* stations from which oxygen data are presented.

Oxygen determination on Cruise 66-A-8 were made by the Winkler method, using potassium bi-iodate as the standard; oxygen data on 67-A-4 and 67-A-8 were determined by the Chesapeake Bay Institute technique for the Winkler method described by Carpenter (1965); and all oxygen determinations for cruises prior to 1966 were made with modifications of the Winkler method.

Figure 1-12 displays plots of dissolved-oxygen concentration versus depth for the basin waters based on the three cruises in 1966 and 1967. Also shown are visually determined best-fit curves. In Figure 1-13, oxygen versus depth is plotted for seven pre-1966 cruises.

For each cruise considered here, Table 1-3 gives the standard deviation and the numerically averaged oxygen concentration, $\overline{O}_2$, for all samples taken at or below 1500 m. There is no evidence that the oxygen concentration changed during the period covered. The oxygen data collected on the 1962 and 1964 cruises show much more scatter at any given depth than do the oxygen data presented from the other cruises. As noted, it is very probable that this scatter resulted from poor sampling or inaccurate analyses. Moreover, horizontally uniform oxygen concentrations are consistent with the horizontal uniformity of salinity and potential temperature observed for the basin waters.

Wüst (1964:45, table 15) has given a value of 5.6 ml/l for the dissolved-oxygen concentration in

Figure 1-12. Oxygen versus depth in the Gulf of Mexico Basin. Plotted are all data from the ⩾ 1400-m sampling depths on the indicated cruises. The solid curves were selected by eye to best fit the data. The dashed curve is for the 67-A-4 data from the Yucatan Basin.

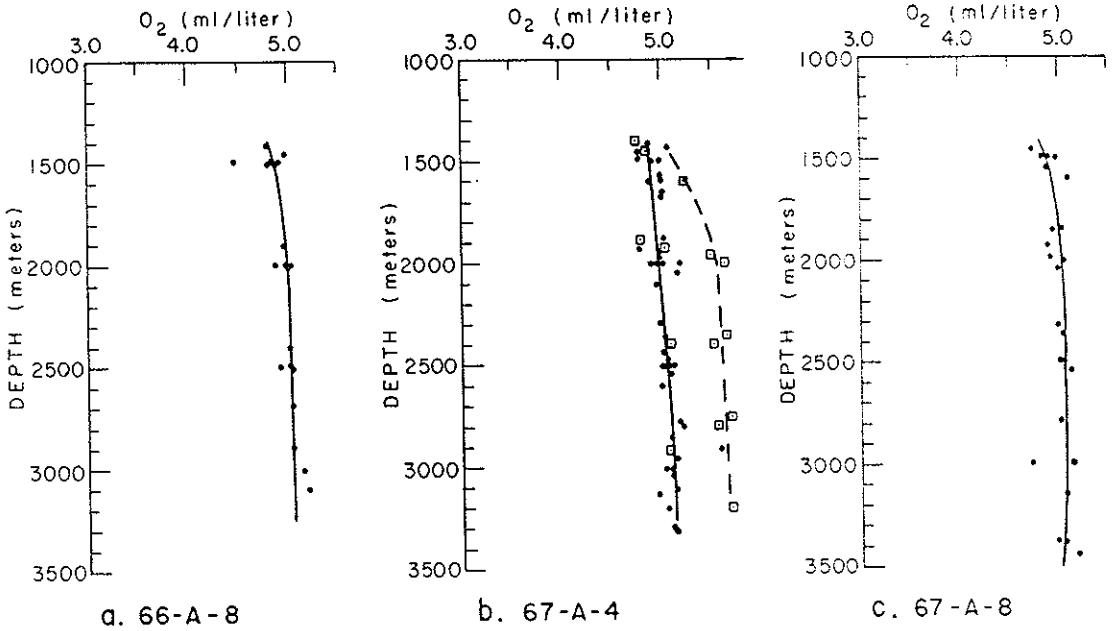

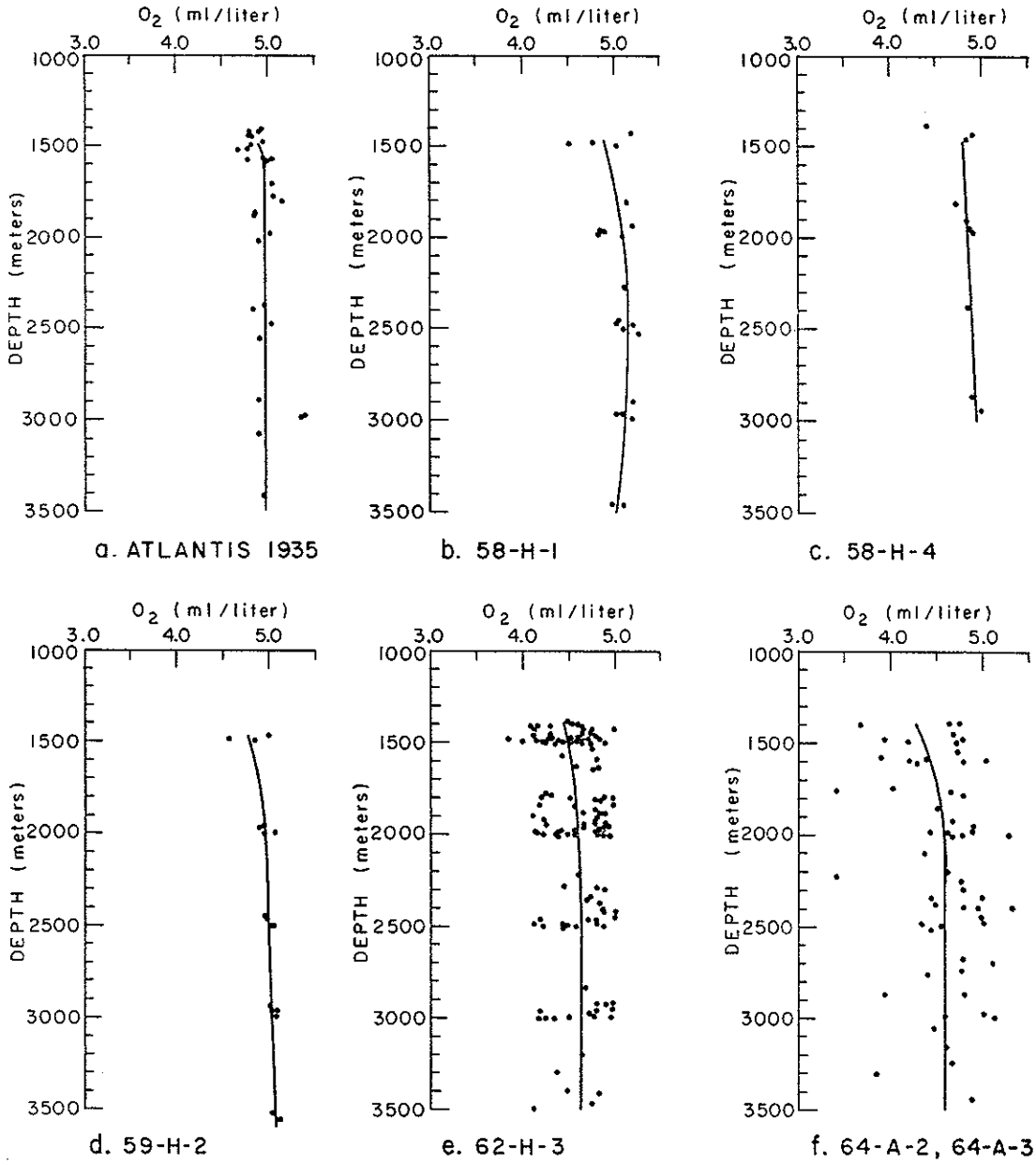

Figure 1-13. Oxygen versus depth in the Gulf of Mexico Basin. Plotted are all the data from the ⩾ 1400-m sampling depths on the indicated cruises. The solid curves were selected by eye to best fit the data.

the deep waters of the Yucatan Basin. This agrees with our value of 5.6 ml/l obtained on Cruise 67-A-4 at two deep stations in the Yucatan Basin near Yucatan Strait (see Table 1-3).

Our mean value for oxygen in the Gulf of Mexico Basin waters is 4.91 ml/l when based on data from the 10 cruises listed in Table 1-3, or 4.99 ml/l if the 1962 data are excluded. Wüst shows values near 5 ml/l within the Yucatan Basin at depths of about 1500-2000 m, i.e., depths from which waters could enter and fill the Gulf of Mexico Basin.

Although the uncertainty in dissolved-oxygen values obtained on Cruise 62-H-3 is large enough to prohibit the use of those data in characterizing oxygen distributions within the basin waters, measurements made on that same cruise can be used to indicate distributions within the overlying waters, in which variations in dissolved-oxygen content far exceed the errors. Figure 1-14 shows typical oxygen-depth curves from the surface to 1250 m. Surface values were found to be generally at or near saturation for the particular temperature and salinity. The most persistent feature is a continuous layer of minimum dissolved-oxygen content. This shows up at depths of about 700 m on the right-hand side of the main Yucatan inflow (Sts. 18 and 20), in the center of the Loop Current regime (Sts. 41 and 55) and in the southerly portion of the outflow (St. 24). To the left of the inflow (St. 15) and of the outflow (St. 26) the minima occur at considerably lesser depths, reflecting the mass adjustment associated with the circulation. Extreme values in this oxygen-minimum core were in the range 2.5-2.7 ml/l, consistent with those shown by Wüst (1964: plate XV), and they are clearly continuous with the core that he traces through the Caribbean (plate XIX). This oxygen-minimum core does not coincide with the salinity-minimum core but occurs at a depth less by some 200 m.

A secondary oxygen minimum at 150-300 m, observed throughout the water bounded by the Loop Current, was almost completely suppressed at St. 26. The shallow maximum and minimum observed at St. 26 are illustrative of a number of such regional features observed in the northern and northeastern part of the survey, especially over the continental shelf. These near-surface maxima, which are not necessarily associated with

Table 1-3
Mean Values of Dissolved Oxygen Concentration Observed in the Basin Waters of the Gulf of Mexico

Cruise	Standard deviation (ml/l)	O_2 (ml/l)	Number of stations ($Z \geqslant 1500$ m)	Number of data points ($Z \geqslant 1500$ m)
Atlantis 1935	0.134	4.96	9	23
58-H-1	0.124	5.08	6	19
58-H-4	0.054	4.87	4	7
59-H-2	0.055	5.01	5	17
62-H-3	0.280	4.62	52	114
64-A-2 and 3	0.482	4.58	19	67
66-A-8	0.048	4.99	7	19
67-A-4:				
Mexico Basin	0.077	5.03	16	55
Yucatan Basin	0.099	5.61	2	11
67-A-8	0.111	5.01	9	21

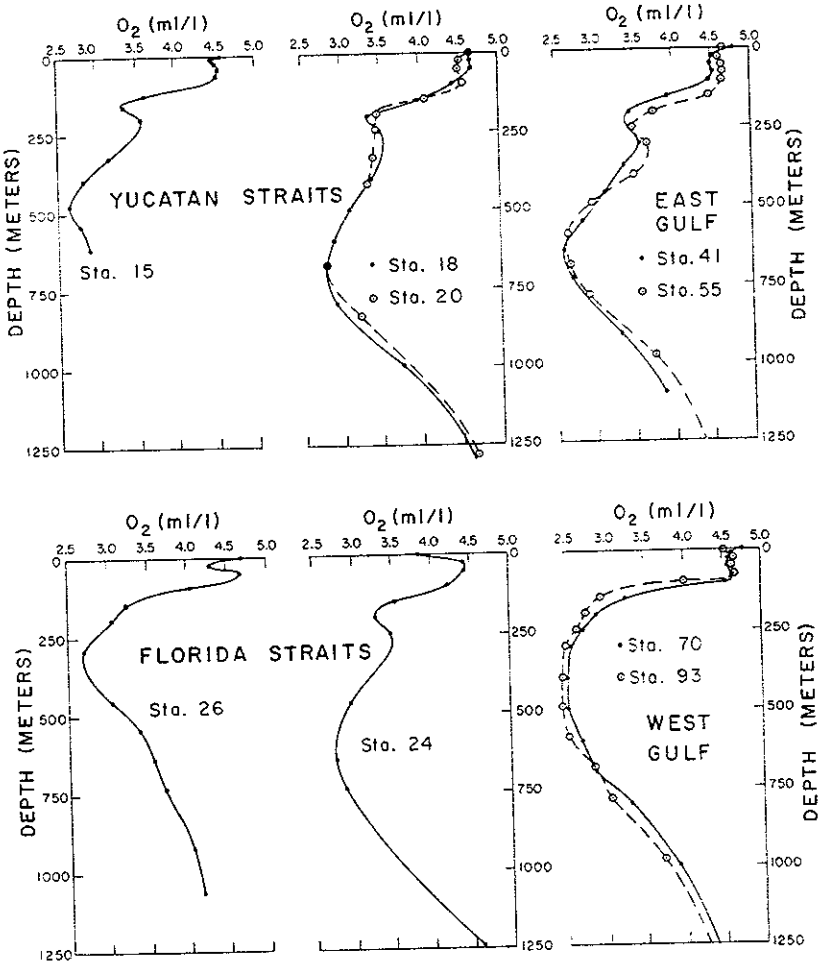

Figure 1-14. Dissolved-oxygen concentration versus depth at selected stations on Hidalgo *62-H-3, Gulf of Mexico.*

corresponding temperature or salinity extrema, are likely associated with biological activity. They are presently unexplained and seem worthy of future investigation.

In the western Gulf (represented by Sts. 70 and 93) the oxygen-minimum layer is considerably thicker, and the lower extreme values (typically 2.4 ml/l or less) indicate a considerable residence time for this water. The oxygen content in vertical profile along Section *D* (approximately 93°W) is shown in Figure 1-15. The maximum vertical gradient of dissolved oxygen occurs between depths of 75-150 m across the section, corresponding to the top of the thermocline (Figure 1-24). The depth variations in the oxygen-minimum layer appear to be related to the circulation, and below this the configuration of oxygen isopleths generally conforms to the isotherms and isosteres (see Figures 1-24 and 1-27). The very low value observed in the minimum layer at St. 105 (1.67 ml/l) suggests the possibility of a permanent eddy in Campeche Bay.

Overlying the basin waters within the Gulf of Mexico are several strata having distinct water mass characteristics indicative of their sources. In addition to the layers (already discussed) in which the concentration of dissolved oxygen has local extrema, there are strata characterized by local maximum values of salinity, minimum values of salinity or (near the surface) vertically uniform concentrations of both salinity and temperature.

Remnant of Subantarctic Intermediate Water

Wüst (1964) has reviewed his earlier (1936) findings concerning the distinctive water mass that is formed near the Polar Front in the South Atlantic (48° -52'S). To this water mass he gave the name Subantarctic Intermediate Water. The mechanism of formation is not well understood, but these waters sink and spread out northward. The core of minimum salinities enters the Caribbean through those passages of the Lesser Antilles that have sufficient sill depth and then spreads out in the Caribbean as shown by Wüst (1964: plates XVI and XVII). Salinities in this core may be less than 34.7 per mil in the eastern Caribbean, but mixing that accompanies the horizontal spreading raises the salinity to 34.85 per mil at the Yucatan Strait.

Figure 1-16 shows the depth of the salinity minimum as observed in the Gulf; it also shows representative salinities and temperatures. Prior to contouring, the depths at each station were selected from smoothed curves of observed salinity versus depth. From the following discussion of currents it will be recognized that the depths are related to the circulation, being greater than 900 m in the center of the water bounded by the Loop Current and close to 500 m in the northern central Gulf.

Figure 1-15. Dissolved-oxygen concentration along vertical Section D, 22-27 March 1962, Hidalgo *62-H-3. Upper 1250 m at interval of 0.2 ml/l. Observation positions indicated by dots. Vertical exaggeration 555:1.*

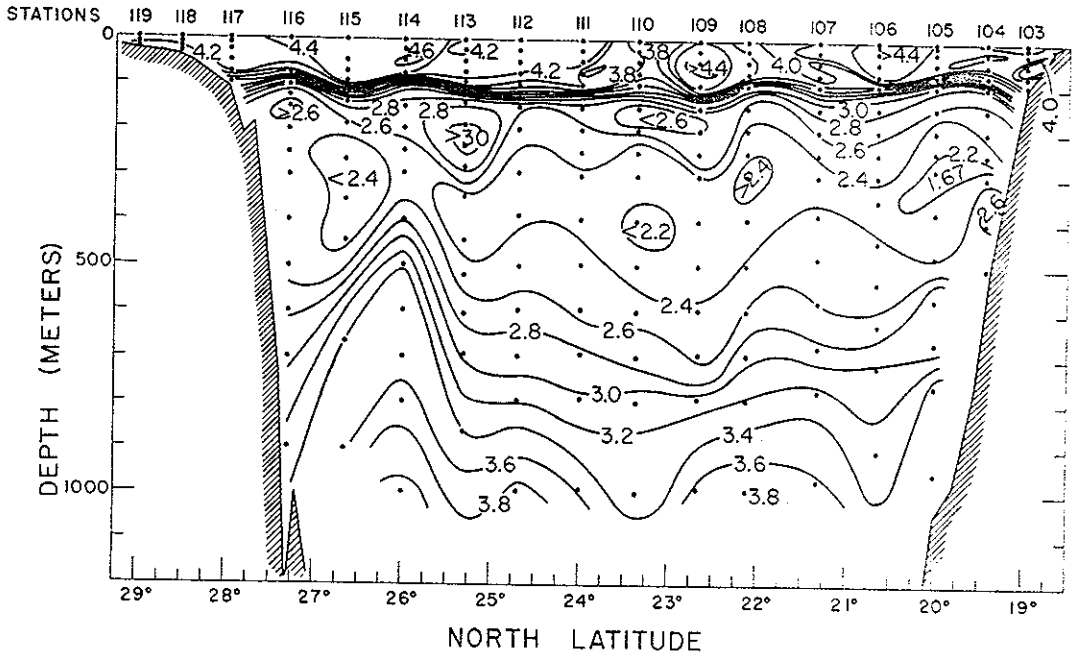

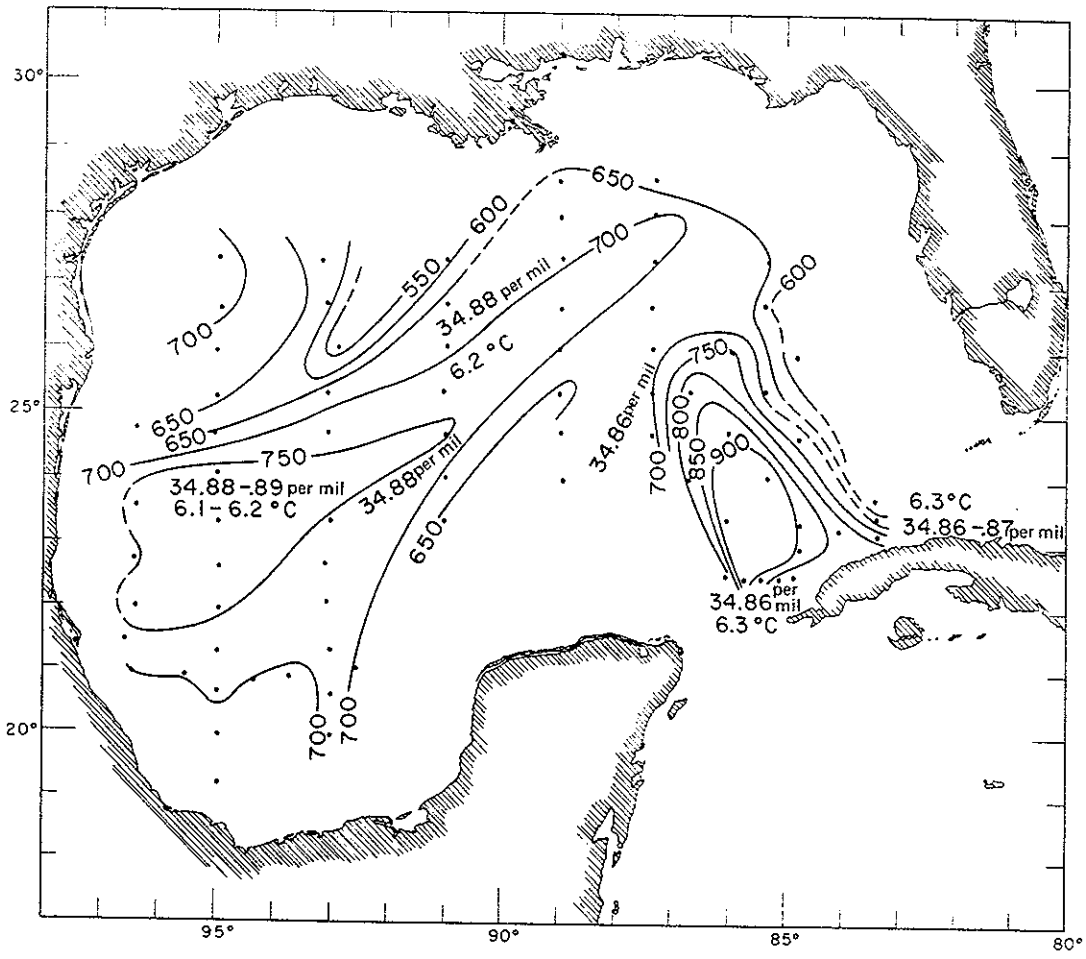

Figure 1-16. Depth (50-m intervals) of core layer in Subantarctic Intermediate Water remnant (salinity minimum), Hidalgo *62-H-3. Selected values of salinity and temperature at the core are shown.*

On the basis of minimum salinity, Wüst (1964) has constructed a table for estimating the percentage composition of the Subantarctic component in the core. This would indicate that at Yucatan (34.86 per mil) there is already less than 5 percent and in the western Gulf (34.88-34.89 per mil) only some 1 or 2 %. Even so, the origin of this distinctive feature of minimum salinity within the Gulf is clear, and it is proper to label it a remnant of the Subantarctic Intermediate Water.

Tropical Salinity Maximum

Another distinct layer in the water structure of the Gulf shows up as a subsurface salinity maximum. Wüst (1964) has traced this layer through the Caribbean and has given it the name Subtropical Underwater. According to him, it originates at the surface-salinity maxima in the North and South Atlantic (cf. Defant, 1961: plate 5), where its maximum surface expressions are found at 20°-25°N, 30°-50°W and at approximately

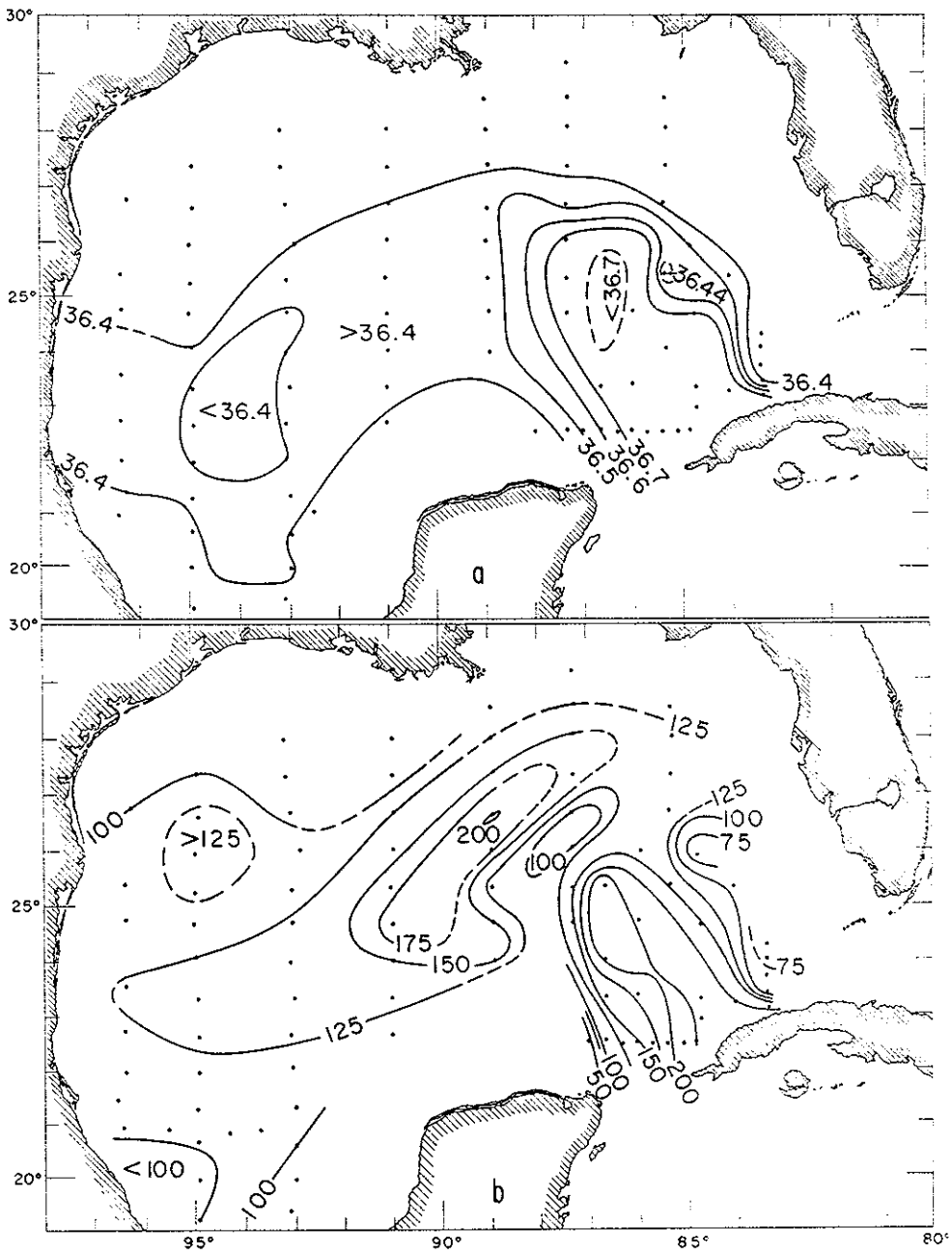

Figure 1-17. Core of salinity maximum, Hidalgo *62-H-3: (a) salinity (0.1 per mil intervals); (b) depth (25-m intervals). Locations of maxima indicated by dots.*

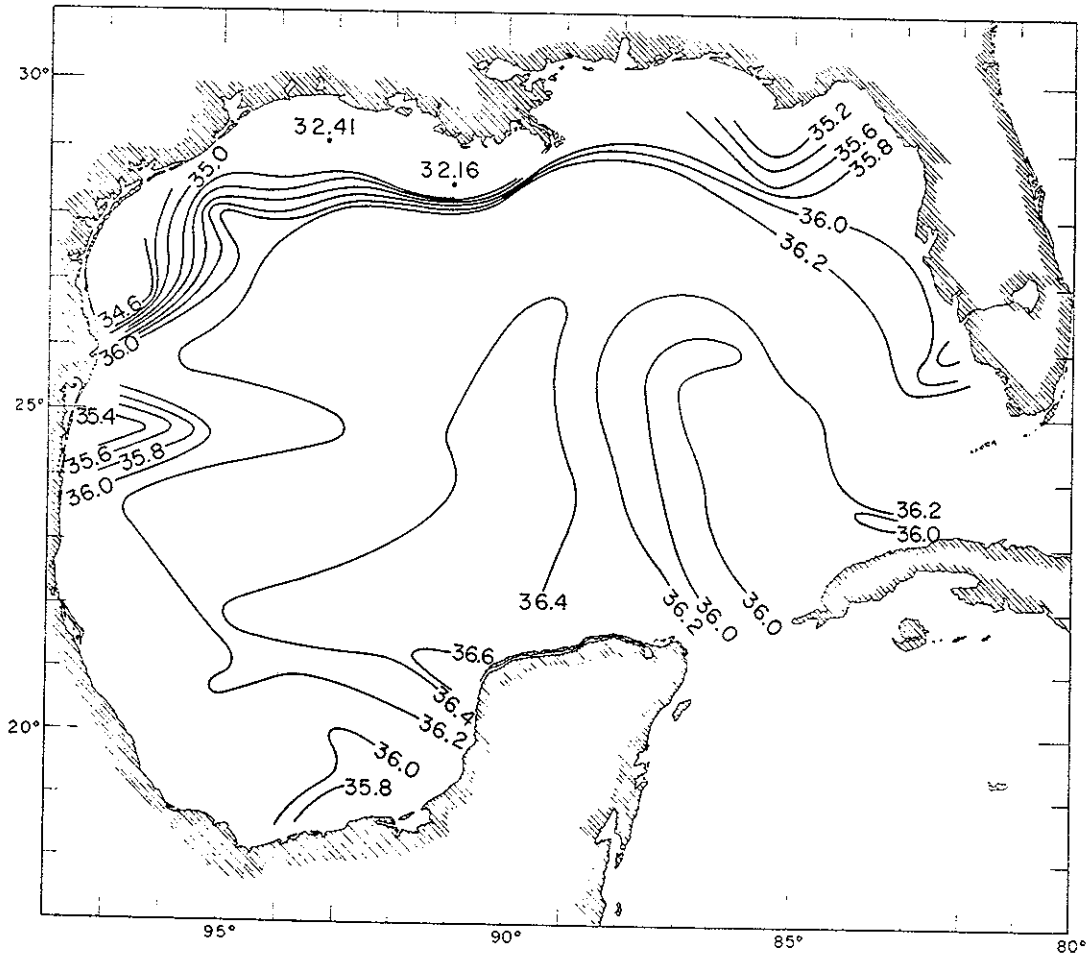

Figure 1-18. Surface salinities (parts per mil), Hidalgo *62-H-3.*

15°S, 30°W; westward these maxima spread out as intermediate layers. Although the core of the South Atlantic component extends along the northern coast of South America, Cochrane's (1965) presentation of data from the EQUACHEQUE Expedition makes it clear that the maximum salinites encountered offshore from northern Brazil are already too low for the South Atlantic to be considered a source for the Subtropical Underwater in the Caribbean. We may point then to the tropical North Atlantic as the source region for this layer in the Caribbean and the Gulf.

Salinity values at the subsurface maxima are shown in Figure 1-17. The maximum salinity in this layer is about 36.75 per mil, in agreement with Wüst (1964: plate XIII), and is confined to the water bounded by the Loop Current. In the western part of the Yucatan Current, the salinity appears to be decreased by vertical mixing, as discussed above. As a consequence, the salinity maxima throughout most of the Gulf are lower than those in the water bounded by the Loop Current. As shown in Figure 1-17, the average depth of this layer is about 150 m, which is in general

agreement with the depths at which the layer is found in the Caribbean.

The Surface Layers

The observed surface salinities are depicted in Figure 1-18; surface salinities taken underway were used to augment station data in constructing this figure. In the Yucatan area and the water bounded by the Loop, the values 35.9-36.2 per mil are typical of the Caribbean during the winter.

An interesting feature of the surface salinity pattern in Figure 1-18 is the relative high (S>36.4 per mil) covering the western Campeche Bank and extending over the deep water areas to the west and north. Salinities near the bank were reexamined in an effort to understand that distribution. During Cruise 62-H-3, salinities along the eastern bank edge exceeded 36.4 per mil (Figure 1-20*b*). It was suspected that high-salinity waters might be moving from the east up onto the central Campeche Bank in a frictional bottom layer (in a manner described by Cochrane, 1967) and then upwelling to give the surface distribution of high salinity shown over the western bank. Although this cannot positively be denied on evidence from Cruise 62-H-3, the data from Sts. 10 and 11 show salinities over the central bank of approximately 36.32 per mil from top to bottom. At the four other Campeche Bank stations salinity was nearly uniform with depth, having values of 36.48 per mil at Sts. 9 and 75, 36.52 per mil at St. 76 and 36.67 per mil at St. 77. Either during or before Cruise 62-H-3, it is possible that a band of high-salinity water, extending south of St. 10, connected the high-salinity surface feature and the high-salinity intermediate waters of the Yucatan Current along the eastern bank edge. The data were also examined for evidence of a connection between the surface high and underlying waters of the subtropical salinity maximum, found west and north of Campeche Bank at depths of 100-150 m. At each station the high-salinity surface was separated from the high-salinity subsurface waters by a relatively lower salinity layer.

Runoff from the Mississippi and Atchafalaya and from smaller rivers to the east and west gives rise to a band of low-salinity water along the northern shore. Most of this water flows westward over the Texas Shelf and shows its freshening influence as far south as 26°N. The tongue of fresher water protruding eastward from the Mexican coast at about 25°N may have been a continuation of the coastal flow augmented by the Rio Grande River, or it may have been entirely due to local runoff. Station spacing was inadequate for a positive interpretation.

The horizontal distribution of average salinities within the upper 50 m presented by Parr (1935: figure 10) from the *Mabel Taylor* data is strikingly similar to the pattern in Figure 1-18, although there are not enough *Mabel Taylor* data to conclusively establish that relatively high-salinity (S>36.25 per mil) surface waters covered the Campeche Bank, as Parr pictured. Parr found surface salinities less than 36.0 per mil over the northern shelves; values less than 24 per mil were observed near the mouth of the Mississippi River. During the winter of 1932, the surface waters in a band southeast of the Yucatan Current and along the northern coast of Cuba had salinities less than 36.0 per mil, just as did the surface waters bounded by the Loop Current in the winter of 1962.

Franceschini (1961) studied the hydrologic balance of the Gulf of Mexico for the year October, 1958, through September, 1959, using meteorological observations from stations around the region as well as observed river discharge rates. He showed the Gulf to be an area where evaporation generally exceeds precipitation, but he found a distinct seasonal variation in computed values of evaporation minus precipitation. During the winter season of 1958-1959, particularly during February and March, the western Gulf experienced a net addition of fresh surface water. In summertime, salinities in excess of those shown for the winter season might therefore be expected and have been observed.

The surface-temperature field (Figure 1-19), constructed from Cruise 62-H-3 bathythermograph and station data, shows mainly a latitudinal variation, with an intrusion of warm water from the Caribbean in the southeast, the periphery of which is marked by strong gradients. Winter cooling in the Gulf generally proceeds stepwise as cold fronts move across the central United States and out over the Gulf, but few of these outbreaks extend completely across the Gulf. Some of the apparent surface-temperature structure is due to weather changes during the survey period, e.g., the southerly extension of isotherms in the west, which resulted from two outbreaks of cold air that occurred just prior to sampling. The cooling season prior to this cruise had not been severe; a comparison of the 1962 temperature data with those collected during the winter of 1964 is presented in the next section.

Temperature and Salinity in Vertical Sections

Figure 1-20 shows the temperature and salinity distributions in Section *A*, the east-west line just north of Yucatan Strait (see Figure 1-1). In addition to station data, temperature observations from bathythermograph lowerings between sta-

Figure 1-19. Surface temperatures (degrees Celsius), Hidalgo *62-H-3.*

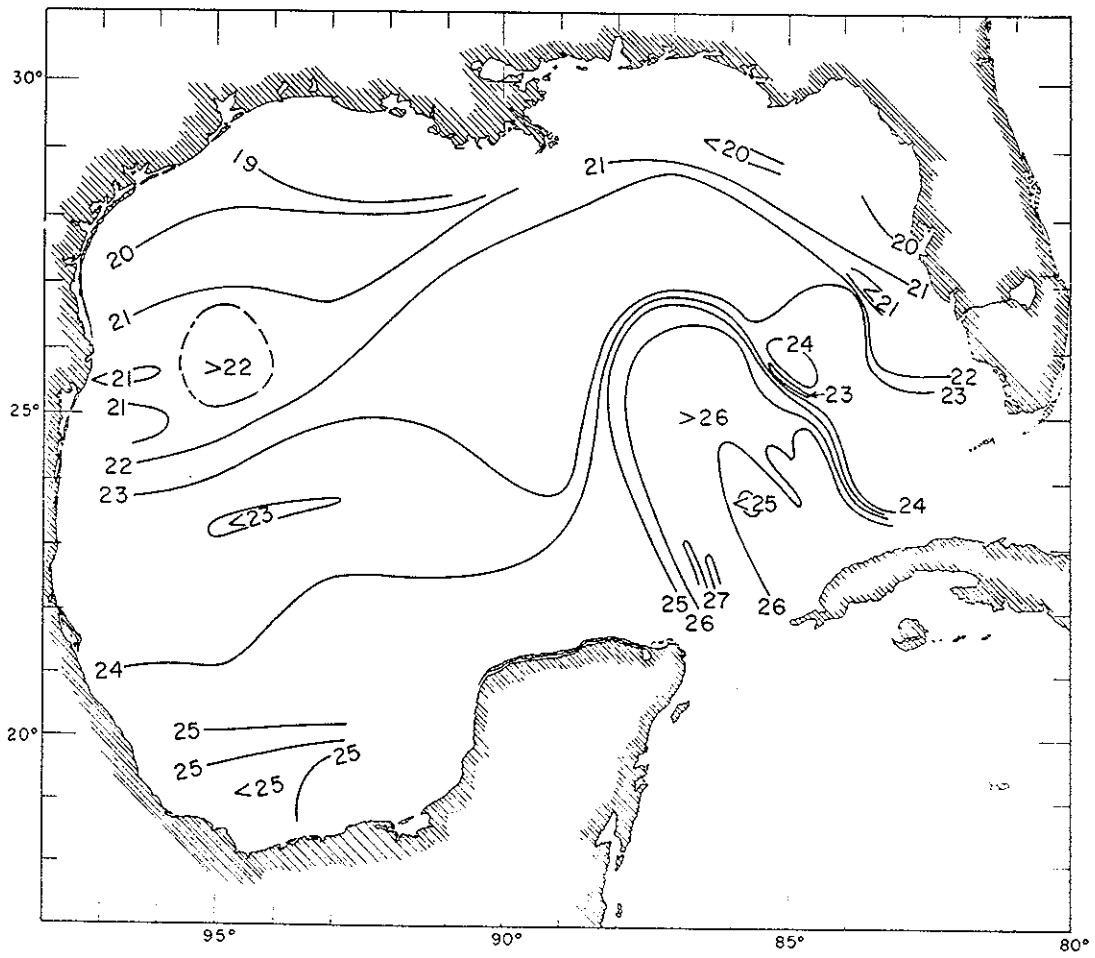

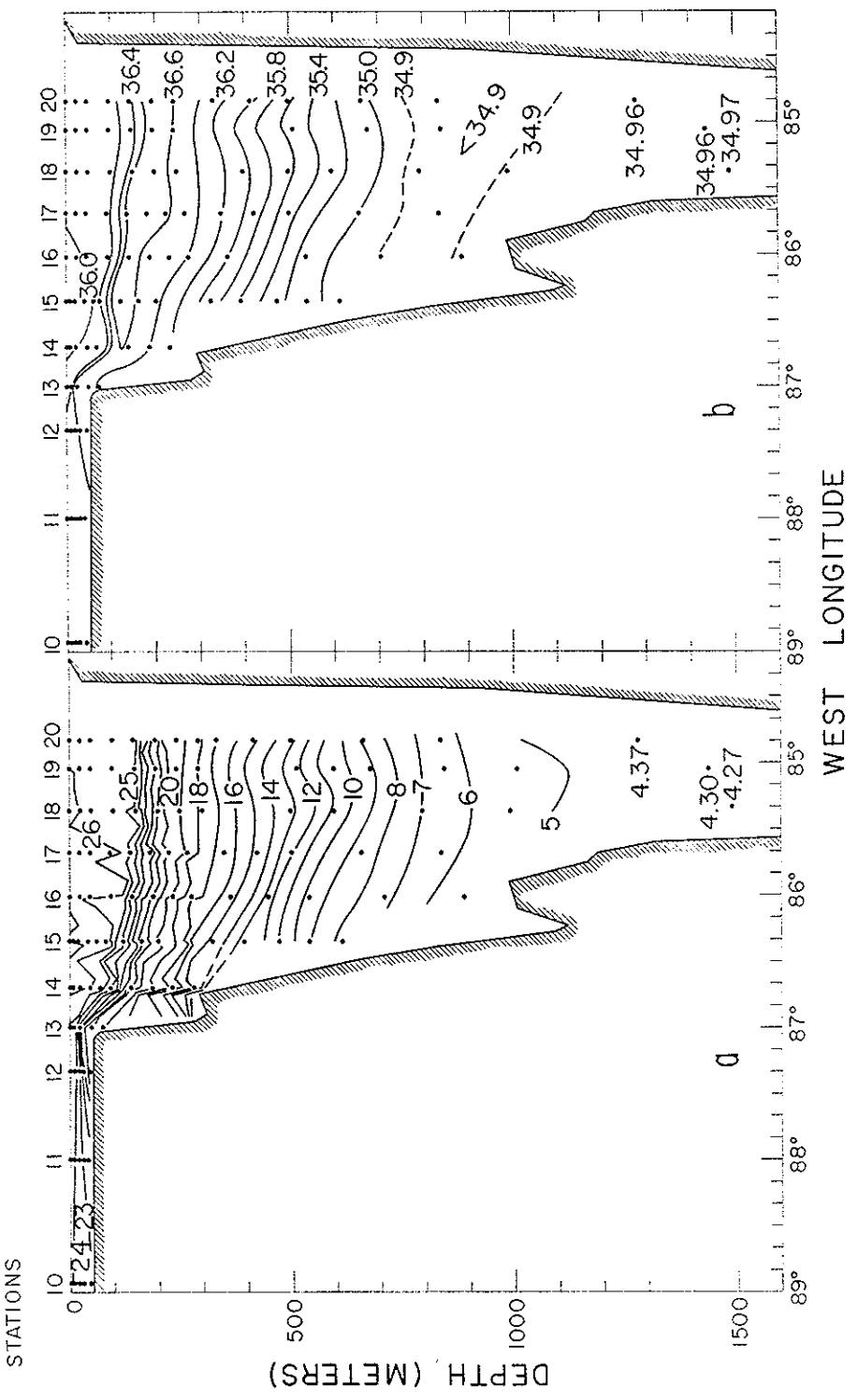

Figure 1-20. (a) Temperature (degrees Celsius) and (b) salinity (parts per mil) along Section A, Hidalgo 62-H-3, 16-18 February 1962. Sampling positions indicated by dots. Vertical exaggeration 340:1.

tions have been used in constructing Figure 1-20, as for each of the vertical temperature sections. Consequently, the isotherms in the upper 275 m show more structure than do the isolines elsewhere in Figure 1-20. The slopes of the isotherms and isohalines indicate northward flow through most of the section; in the western part some northward flow is indicated to at least 1000-m depth or to the bottom. (Here, as in the discussion of vertical sections to follow, the distributions of temperature and salinity are used to infer roughly the currents within the upper 1000 m, with the tacit implication that such flow is relative to an assumed reference level at greater depth.) Southward flow is suggested between Sts. 18 and 19. The thermal structure indicates that there is a marked intensification of the Yucatan Current along its westward flank, with a maximum just to the west of St. 14. East of St. 14 the flow slackens and again increases to another maximum near St.

Figure 1-21. Temperature (degrees Celsius), Section B, Hidalgo *62-H-3. St. 11 occupied 16 February 1962; Sta. 40 through 46, 25-27 February 1962. Sampling positions indicated by dots. Vertical exaggeration 555:1.*

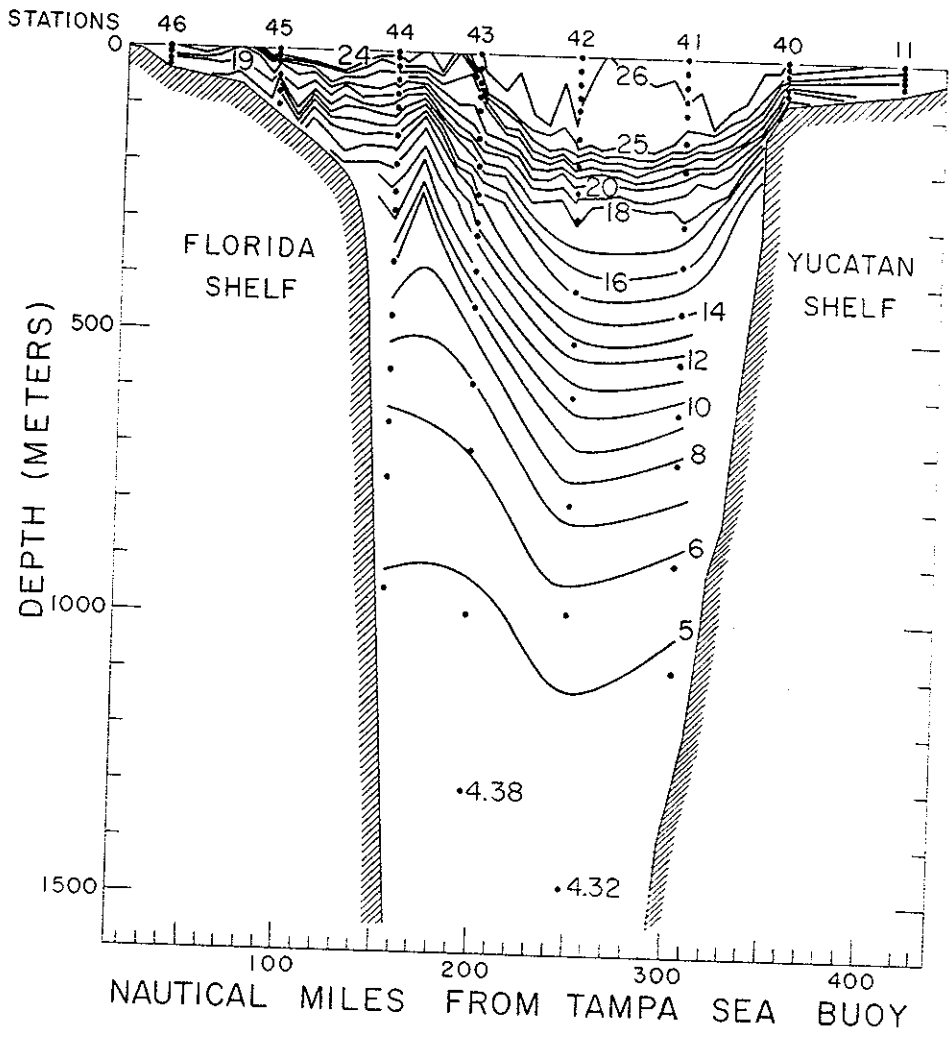

15. Cochrane (1963, 1965) has shown this sort of banded structure to be a consistent feature of the Yucatan Current. Note that, as a consequence of the current structure, waters over the shallow Campeche Bank are of considerably lower temperature and higher salinity than elsewhere at comparable depths.

Figures 1-21 and 1-22 show, respectively, temperature and salinity distributions in Section *B*, from the western Florida Shelf to the Campeche Bank. The subsurface salinity minimum at shallow depths over the Florida Shelf is a feature observed in much of this region. The configuration of isolines shows the two crossings of the major current loop. Bathythermograph data, again used in Figure 1-21, give evidence of a strong flow, with a northwestward component just northeast of St. 40 and a strong southeastward flow in the region of St. 43. Thermal data indicate a region of strong horizontal shear between Sts. 43 and 44, as do the GEK current measurements presented below.

Figure 1-22. Salinity (parts per mil), Section B, Hidalgo *62-H-3. St. 11 occupied 16 February; Sts. 40 through 46, 25-27 February 1962. Sampling positions indicated by dots. Vertical exaggeration 555:1.*

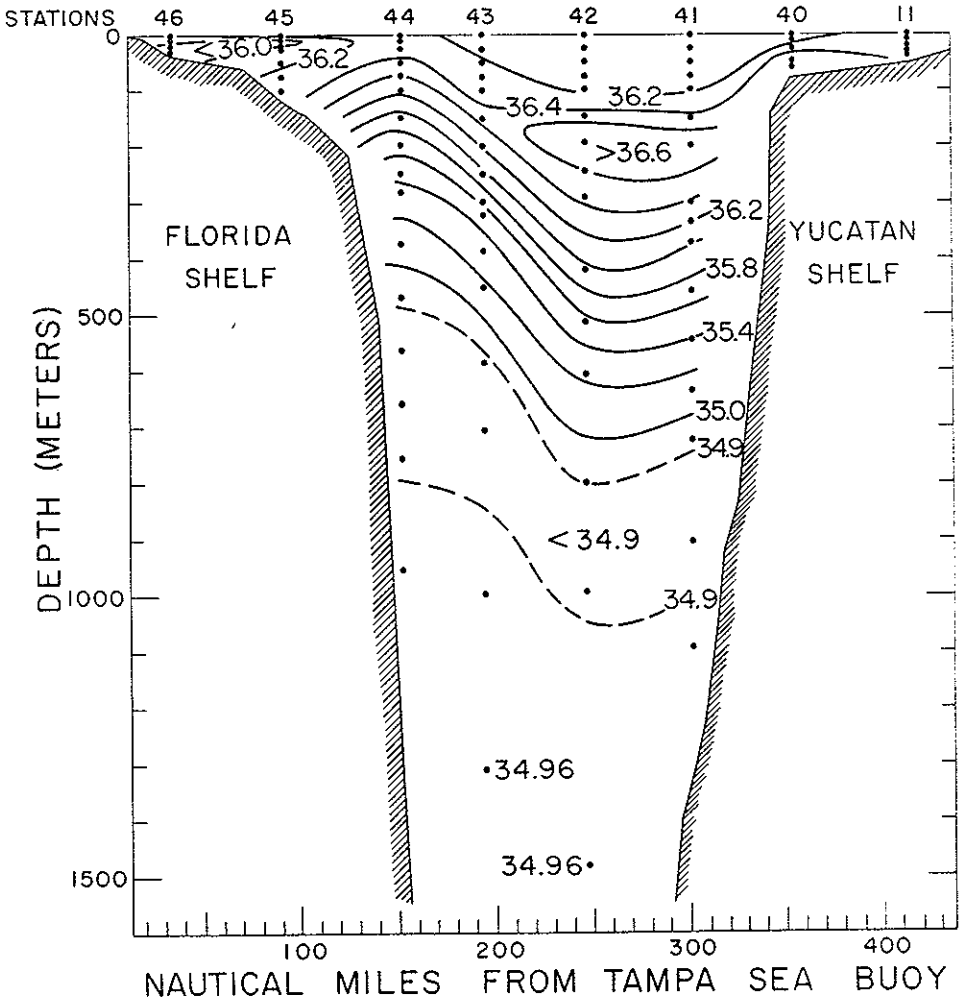

Figure 1-23. (a) Temperature (degrees Celsius) and (b) salinity (parts per mil), Section C, Hidalgo *62-H-3, 19-20 February 1962. Sampling positions indicated by dots. Vertical exaggeration 555:1.*

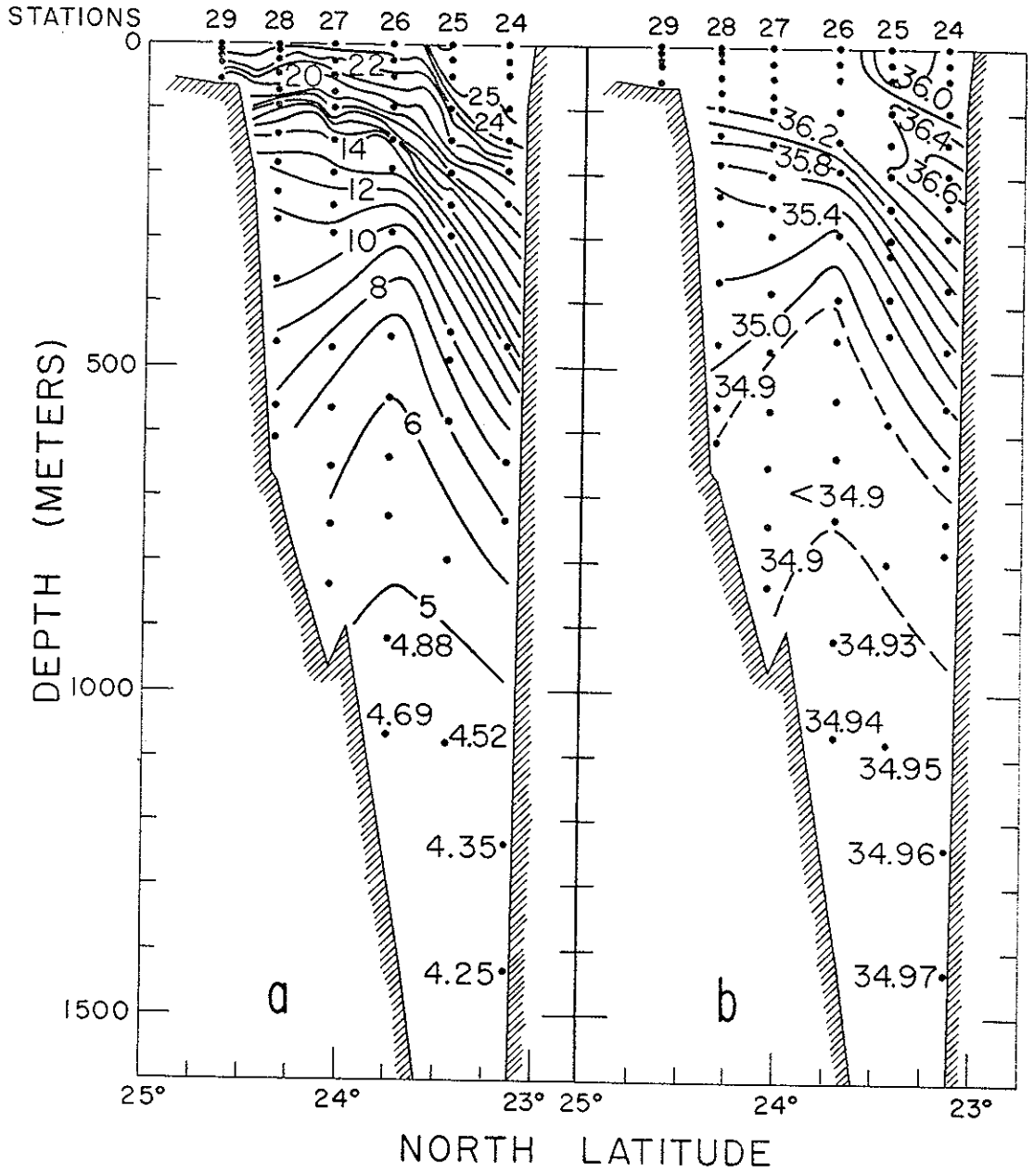

Temperature and salinity for Section *C* are shown in Figure 1-23. The slopes of isolines indicate a strong eastward surface current close to the southern end of the section and some eastward flow reaching to at least 1000-m depth. The flow appears to be reversed (based on the slope of isolines in the deeper waters) in the northern half of the section.

Figures 1-24 and 1-25 show temperature and salinity in Section *D* (93°W). In this section the tropical salinity maximum is only a weak feature. The striking feature of the salinity distribution in the near-surface layers is the occurrence of low-salinity waters, resulting from continental drainage, over the inshore portions of the shelves at each end of the section. The finer scale temperature structure in the upper layers suggests that the flow between the northern shelf and 26°N is not a simple current structure, although a generally westward flow appears to exist to a considerable depth between Sts. 114 and 116. Between Sts. 114 and 112 there is indication of a strong eastward flow based on the configurations of isotherms and isohalines below the thermocline.

The temperature pattern in Figure 1-24 may be compared with that in Figure 1-26, which was taken along approximately the same longitude in late January and February, 1964. The most striking difference is in the extent of development of the mixed surface layer. The thermocline lay almost 100 m deeper in 1964 than in 1962, and the waters above it were cooler and more uniform.

Again in 1964 there was evidence (24°-25°W) of an eastward flow extending to a considerable depth south of the Texas Shelf. However, the current seems to have been centered farther south in 1964 than in 1962. A westward flow near 22°N is indicated for both years. Although these features were less well developed in 1964 than in 1962, and although the eastward flow near 25°N was not in the same location during both years, it is tempting to suggest that there is a regularity in the circulation pattern of the western Gulf. This concept is explored at some length in a succeeding section of this chapter.

Density (σ_t) for Section *D* is shown in Figure 1-27. The features discussed in connection with the temperature and salinity fields are apparent. In the thermocline the maximum stability was typically 1.5-2.0 x $10^{-5}m^{-1}$, with an extreme value of about 3.5 x $10^{-5}m^{-1}$ at St. 105. Below the thermocline, stability decreased monotonically with increasing depth, having values of about $10^{-6}m^{-1}$ at 500 m and 5 x $10^{-8}m^{-1}$ at 1000 m. Below sill depth the stability decreases even further to average values presented in Table 1-1.

Low-Salinity Waters over the Texas-Louisiana Shelf

Figure 1-28 shows the salinity distributions in north-south vertical sections over the outer shelf of the northwestern Gulf. Waters of salinity less than 35 per mil were observed as far west of the Mississippi River as St. 126. Apparently such water, formed by the mixing of river discharge and near-shore waters, is confined to a band along shore some 40-60 nautical miles (75-110 km) wide. Lower salinities were observed at the near-shore locations closest to the Mississippi, which points to this river as the chief source and indicates a general westward spreading. The configurations of isohalines over the outer Texas Shelf, reflected in the density distribution (Figure 1-27), indicate a strong westward flow associated with this low-salinity water.

A similar situation was observed in January, 1966 (Nowlin, unpublished data taken on *Alaminos* Cruise 66-A-1), when a band some 30 nautical miles (55 km) in width containing salinities of less than 35 per mil lay along the coast from Southwest Pass on the Mississippi Delta to at least 95°20'W (the western limit of the survey). During this latter survey the coastal waters (at the 12-m isobath) had salinities of approximately 30 per mil over this region, with the exception of the immediate vicinity of Southwest Pass, where salinities approaching 22 per mil were observed.

In sharp contrast, the January and February, 1964, data taken along 93° and 95°W on *Alaminos* Cruises 64-A-2 and 64-A-3 show no surface salin-

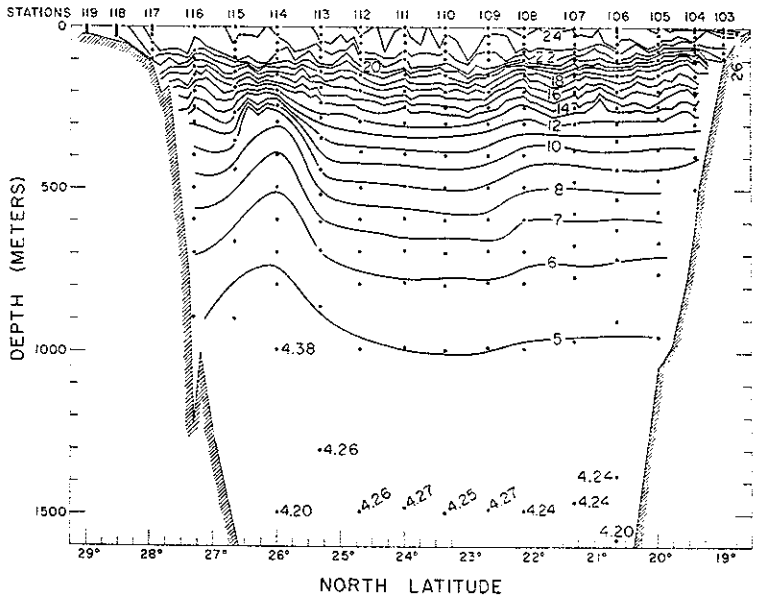

Figure 1-24. Temperature (degrees Celsius), Section D, Hidalgo *62-H-3, 22-27 March 1962. Sampling positions indicated by dots. Vertical exaggeration 555:1.*

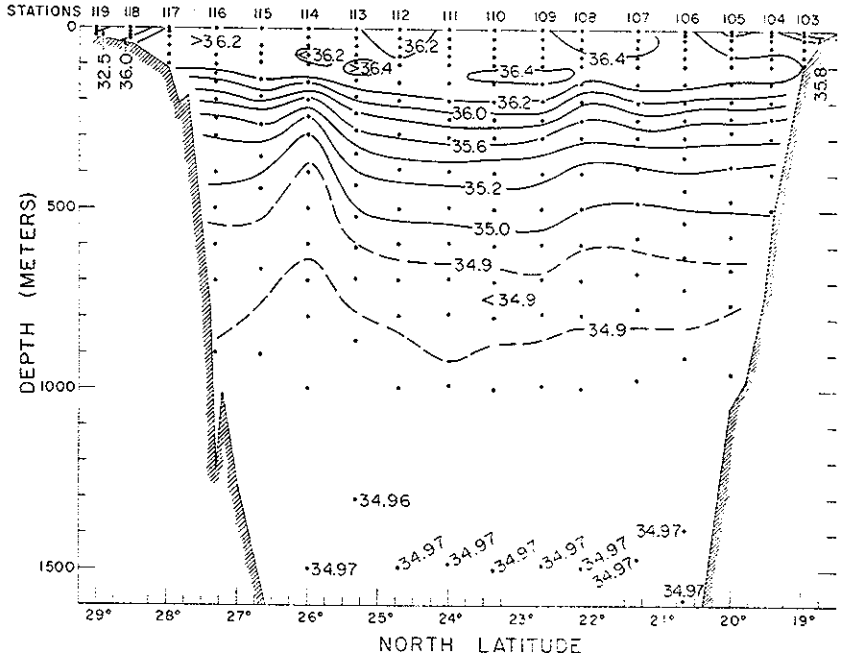

Figure 1-25. Salinity (parts per mil), Section D, Hidalgo *62-H-3, 22-27 March 1962. Sampling positions indicated by dots. Vertical exaggeration 555:1.*

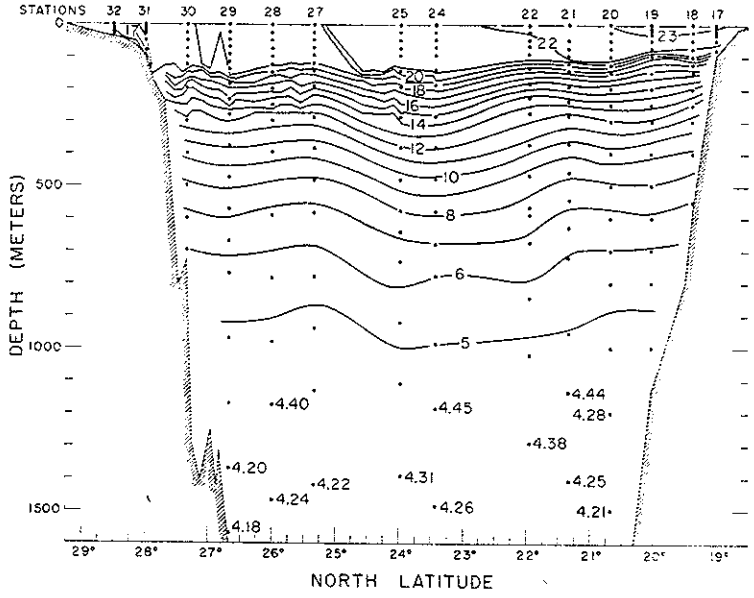

Figure 1-26. Temperature (degrees Celsius) along 93°W (approximately Section D*), Sts. 17 through 21, 24-25 January 1964,* Alaminos *64-A-2; Sts. 22 through 32, 27 February-2 March, 1964,* Alaminos *64-A-3. Sampling positions indicated by dots. Vertical exaggeration 555:1.*

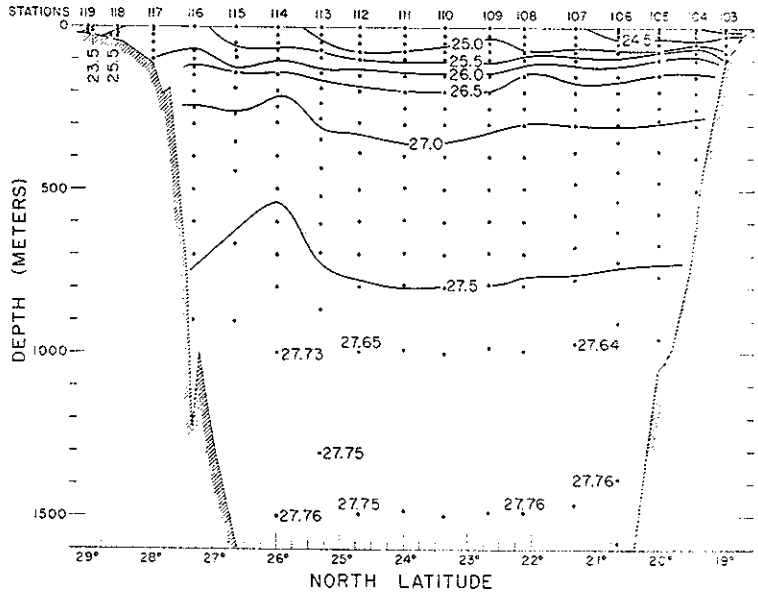

Figure 1-27; σ_t *along Section* D, Hidalgo *62-H-3, 22-27 March 1962. Sampling positions indicated by dots. Vertical exaggeration 555:1.*

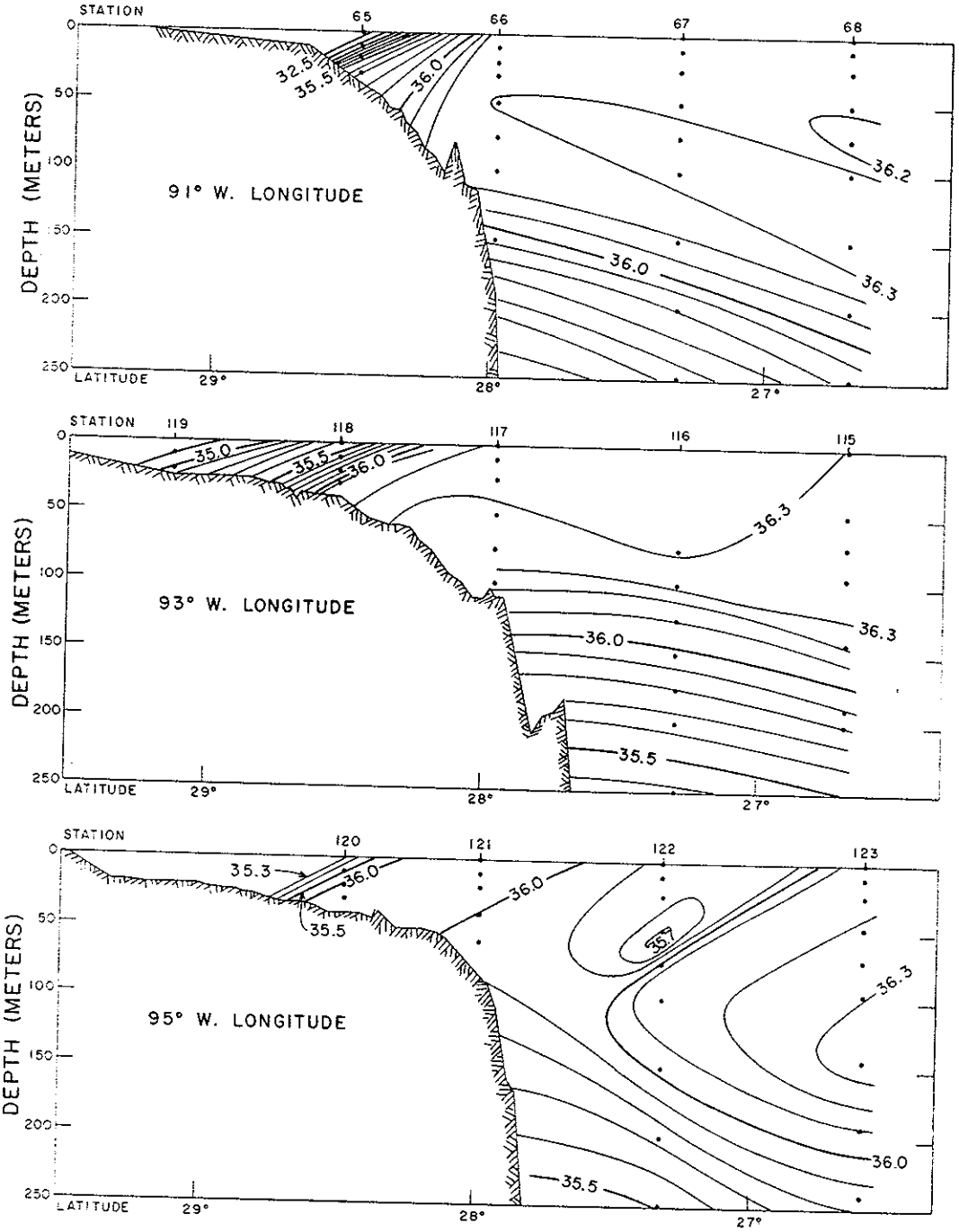

Figure 1-28. Vertical sections of salinity (parts per mil) over outer Texas Shelf, Hidalgo *62-H-3. Data from section along 91°W collected 7-8 March 1962; data along 93° and 95°W collected 26-30 March 1962. Sampling positions indicated by dots. Vertical exaggeration 555:1.*

ities lower than 36.5 per mil beyond the closest station to the shore (35 nautical miles; 65 km).

Currents and Transports

Gross Features

Circulation patterns at the time of the 1962 cruise may be inferred from GEK surface-current measurements and from observed distributions of physical properties. To draw inferences about the current and transport regimes, we have tacitly assumed geostrophic flow and relied on dynamic calculations, even though there may be strong arguments against applying such an assumption to a confined region such as the Gulf.

The dynamic topography of the sea surface relative to the 1000-db surface (Figure 1-29) pictures the Loop Current of the eastern Gulf as the main feature of the surface circulation. The one large eddy centered 60-80 nautical miles (110-150 km) north of the western tip of Cuba, within the confines of the Loop Current, is so often present that some have considered it to be a semi-permanent feature, although we now know that such eddies or rings sometimes become detached

Figure 1-29. Dynamic topography of sea surface relative to the 1000-db surface. Hidalgo *62-H-3;* x's *indicate some extrapolation. Contour interval, 0.05 dynamic meters.*

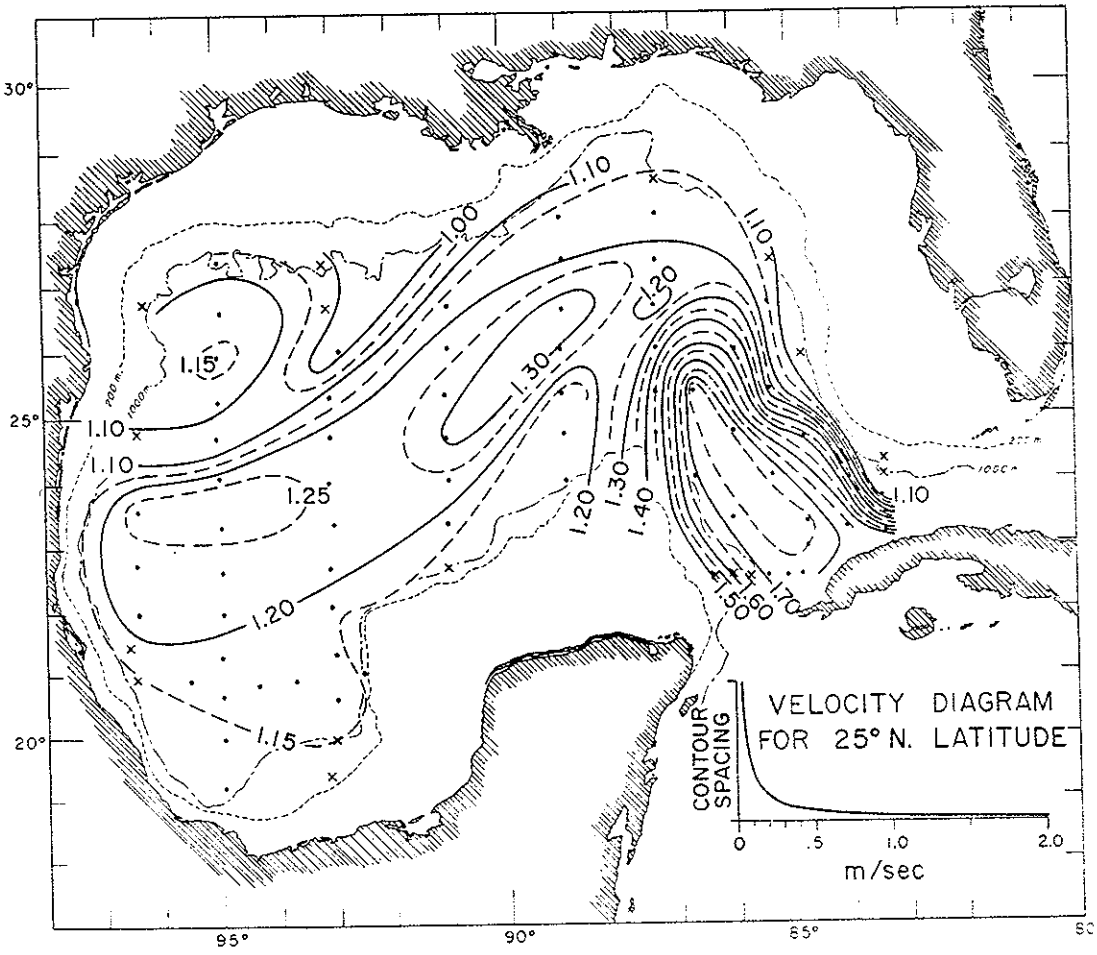

from the main body of the Loop Current. The other principal feature shown in Figure 1-29 is the elongated cell oriented northeast-southwest over the central and western Gulf. That these two anticyclonic circulation systems dominate the circulation in the deep-water regions is also reflected in the mass and property distributions as previously discussed.

In constructing Figures 1-29 and 1-33, some extrapolation was employed for stations at which the maximum sampling depth was between 800 m and 1000 m. In these cases the geopotential anomalies at the maximum pressure sampled, relative to 1000 db, were computed for the two closest deep stations and were then averaged and added to the anomaly for the station in question. The locations of such stations are indicated by *x*'s rather than dots. In constructing Figure 1-32, an analogous procedure was used in extrapolating a few values to 1500 db.

The circulation pattern presented here for the deep-water regions is much simpler than those pre-

Figure 1-30. Dynamic topography (in dynamic meters) of the sea surface relative to the 1000-db surface, Mabel Taylor, *24 January-27 April 1932.*

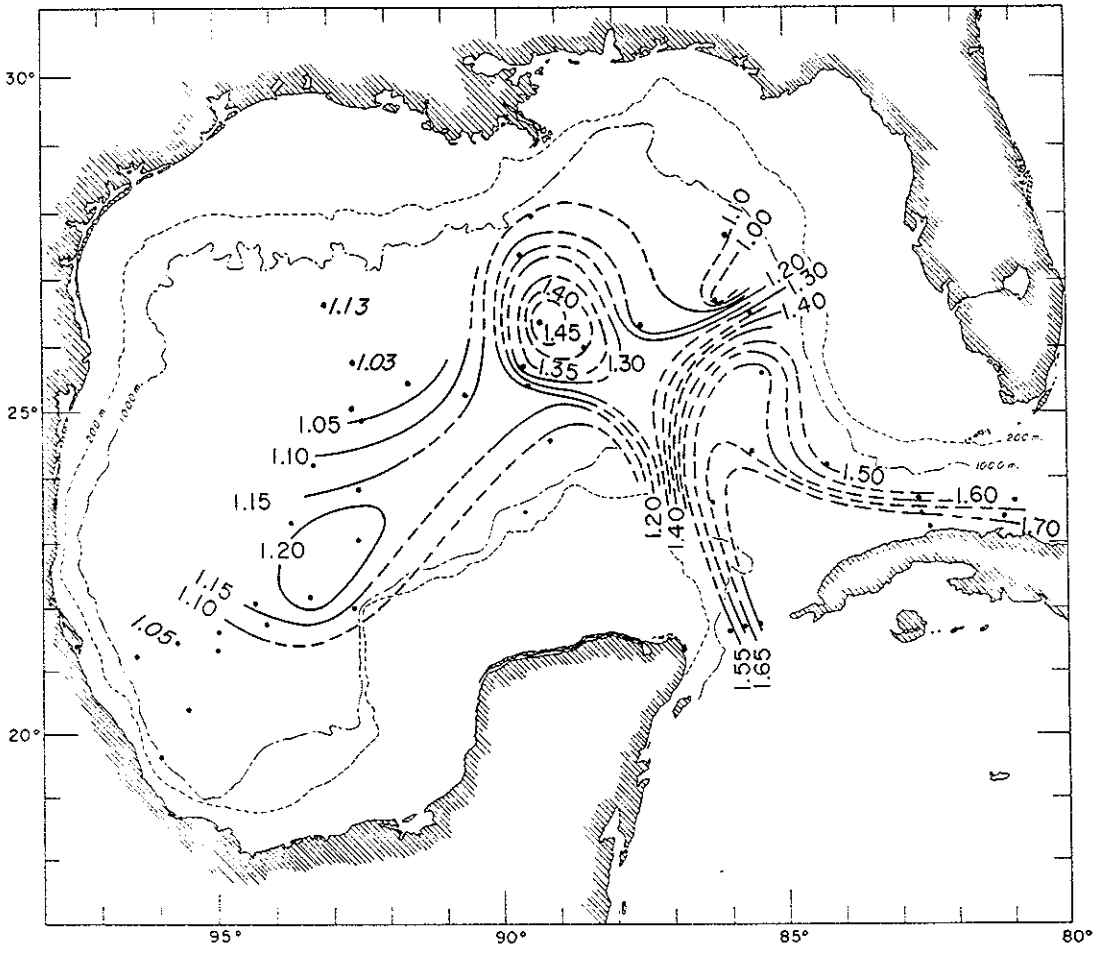

sented by some previous investigators, e.g., Austin (1955) or Duxbury (1962). For comparison with the 1962 data, the 0-db/1000-db geopotential anomalies were computed from data taken during the 25 January-27 April 1932 survey of the Gulf by the *Mabel Taylor* (Parr, 1935) and during the 15 February-13 April 1935 survey by the *Atlantis*. It was found that in both cases the geopotential anomalies could be contoured, with no strain of the imagination, to form patterns (Figures 1-30 and 1-31) consisting of only the same two general features that are evident in Figure 1-29, although the elongated cell in the western Gulf was slightly displaced. The *Mabel Taylor* data have been contoured to emphasize continuity of the high in the central Gulf with that within the Loop Current rather than with the elongated cell over the western Gulf.

Consideration was given to the use of a reference level arrived at by the method of Defant (1961), but I was not able to construct a unique surface with a reasonable depth range in this way.

Figure 1-31. Dynamic topography (in dynamic meters) of the sea surface relative to the 1000-db surface, Atlantis, 15 February-13 April 1935.

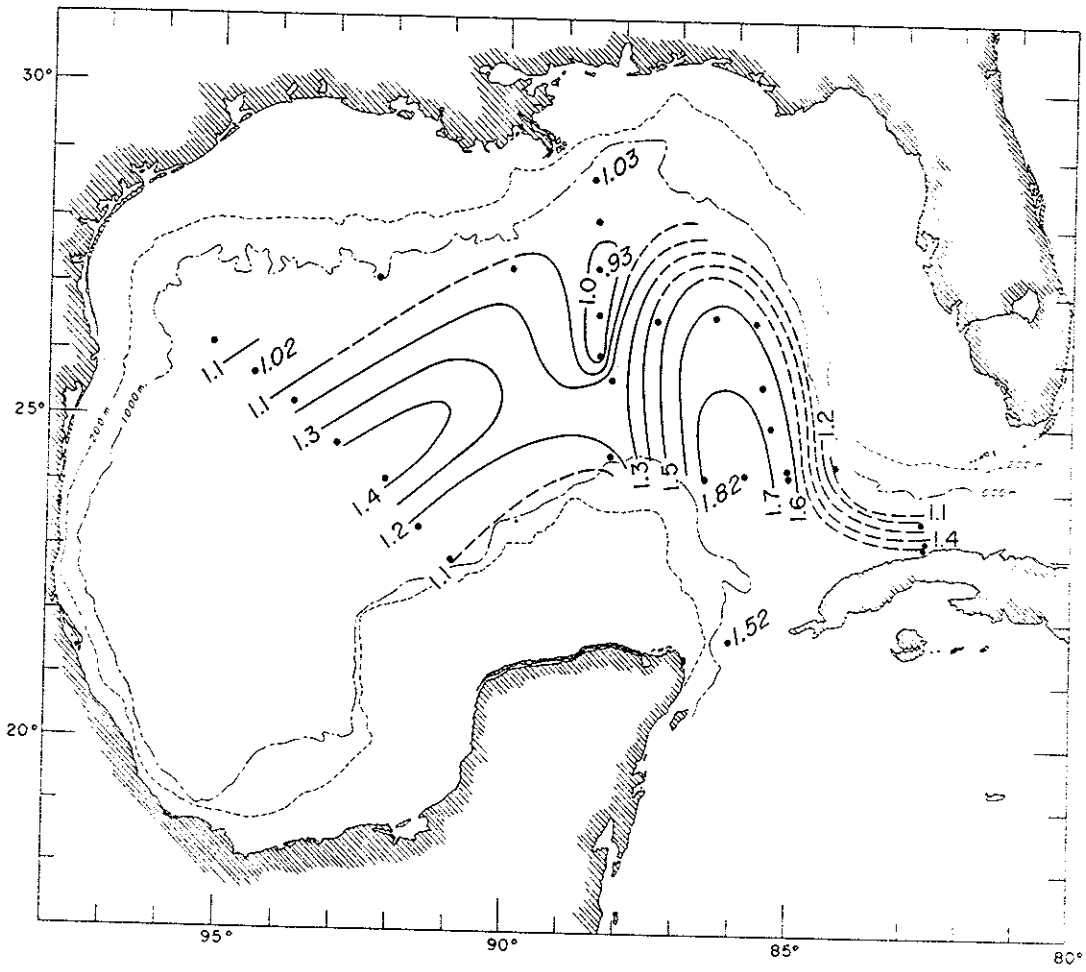

Since the 1962 data showed very little baroclinicity below sill depth, a reference surface below this depth was also considered, but the additional stations lost in the computation made this unattractive.

Geopotential anomalies of the 1500-db surface relative to 2000 db (not shown) indicated a very weak clockwise circulation cell in the western central Gulf and no distinct pattern in the eastern and central Gulf. Gradients on this surface were small, an isolated extreme value being approximately 0.0002 dyn m per nautical mile, which corresponds to a relative current speed of only some 2 cm/sec. Even so, it is interesting to note the indication of some relative motion at and near the sill depth of the basin.

The geopotential anomalies of the 1000-db surface relative to 1500 db (Figure 1-32) show motion with a pattern very much like that in Figure 1-29. However, in the eastern Gulf there is

Figure 1-32. Dynamic topography of the 1000-db surface relative to the 1500-db surface, Hidalgo *62-H-3; x's indicate some extrapolation. Contour interval, 0.005 dynamic meters.*

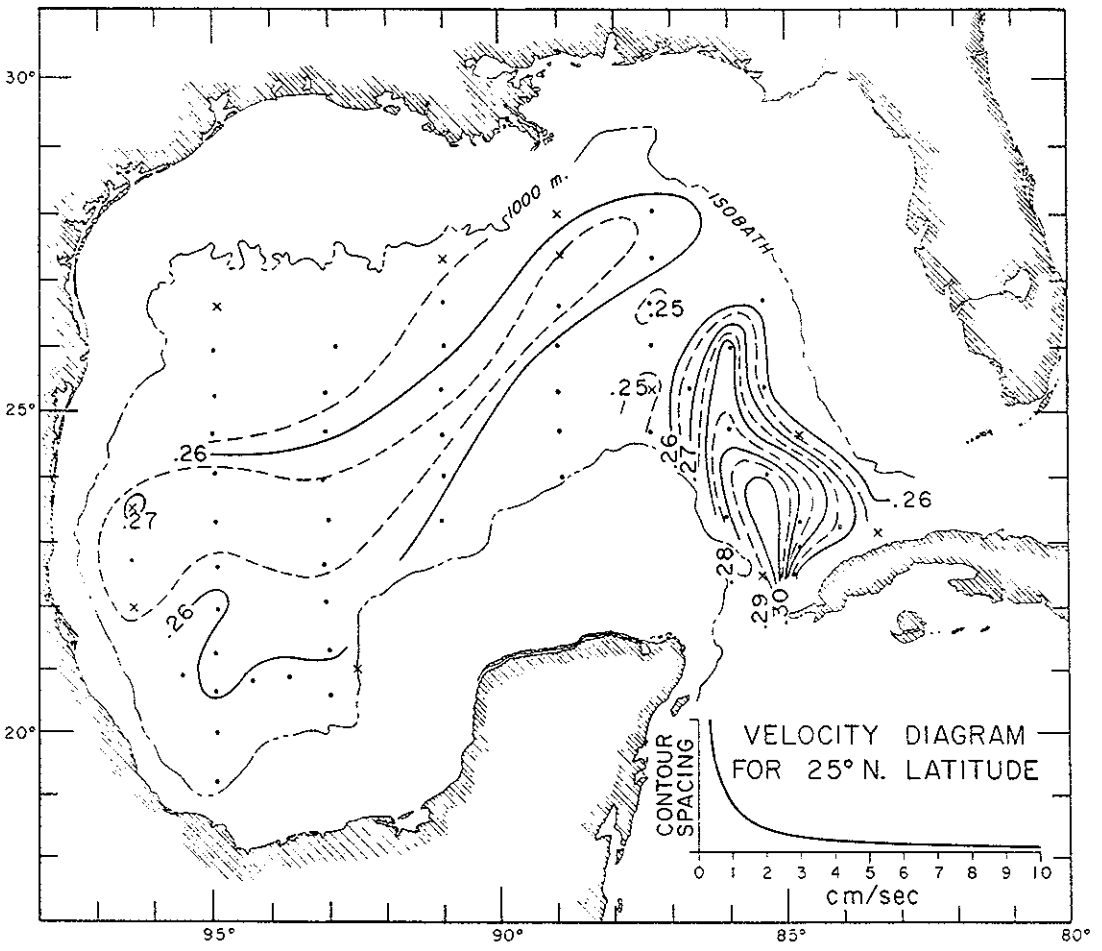

a loop of current that both enters and leaves the Gulf through Section *A* (Figure 1-32). Perhaps this is to be expected, since the controlling depth in the Straits of Florida is thought to be some 800 m (Defant, 1961). This pattern may be partially closed in the Yucatan Strait south of Section *A*. Relative speeds indicated in Figure 1-32 are mostly less than 10 cm/sec. The 1000-db surface may then be taken as a reference for computing geostropic current speeds in the upper layers of the Gulf without introducing errors of much more than 10 cm/sec.

Figure 1-33 presents the contours of geopotential anomaly for the 500-db surface relative to 1000 db. There was considerable motion down to 500 m, and the circulation patterns at the sea surface and at 500 db were quite similar.

Figure 1-34 shows surface currents as inferred from a GEK. No corrections other than those for magnetic-field intensity have been made to these

Figure 1-33. Dynamic topography of the 500-db surface relative to the 1000-db surface, Hidalgo *62-H-3; x's indicate some extrapolation. Contour interval; 0.025 dynamic meters.*

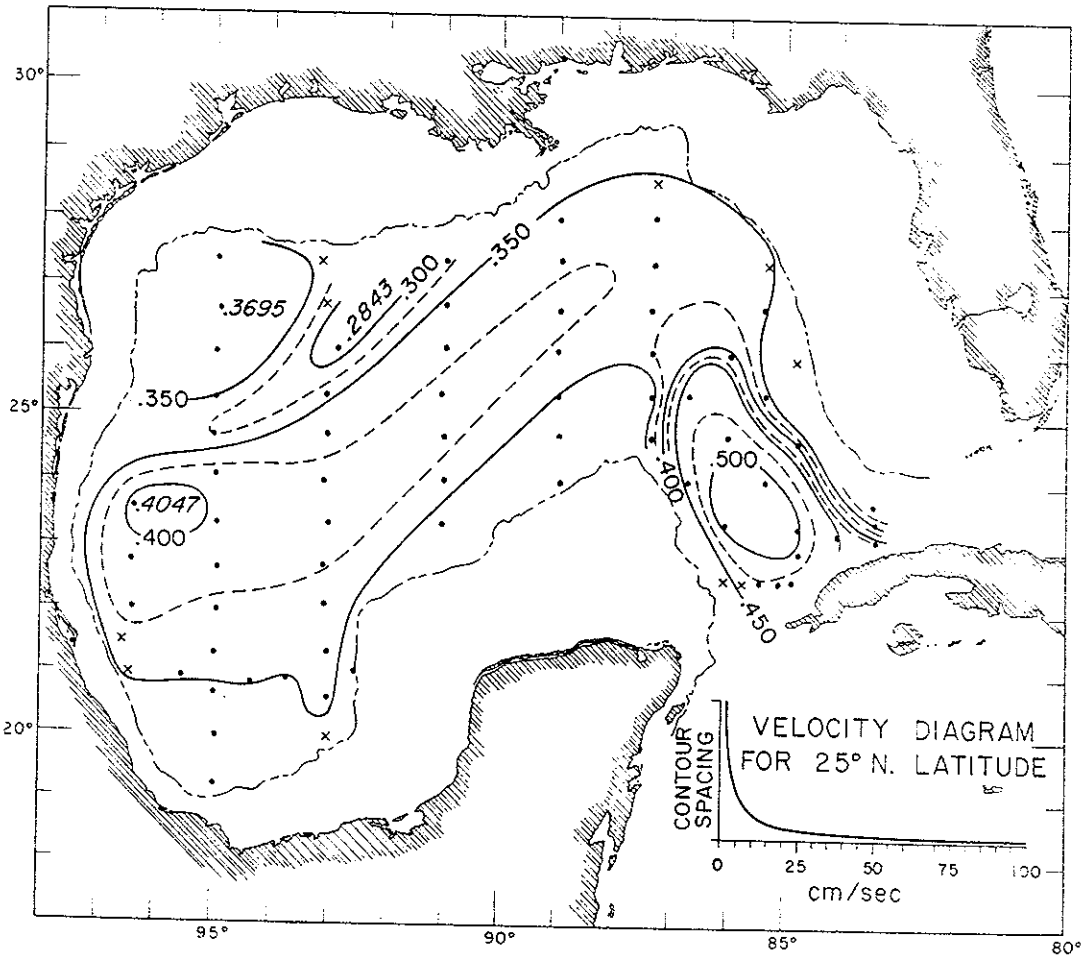

values. Unfortunately, no GEK data were obtained along 89°W.

The GEK measurements are in general agreement with the major features of the computed surface-current pattern. The core of the Loop Current in the eastern Gulf is clearly seen in Figure 1-34. Along the northern boundary of the anticyclonic ridge in the western central Gulf, the core of the northeastward flow is seen, as are the shear zone to its north and the southwestward flow along the outer shelf. The GEK observations show no strong currents along the position of the southern boundary of this ridge, which may be a broad diffuse flow as indicated in Figures 1-29 and 1-33. Many smaller-scale features appear in the GEK data, but these are presumably averaged out or are otherwise not seen in the dynamic topographies.

The geostrophic transport field for the upper 1000 m relative to 1000 db is presented in Figure 1-35. For each station from 1000 m to the surface the geopotential anomaly relative to 1000 db was vertically integrated to obtain the transport po-

Figure 1-34. GEK surface-current observations, Hidalgo *62-H-3.*

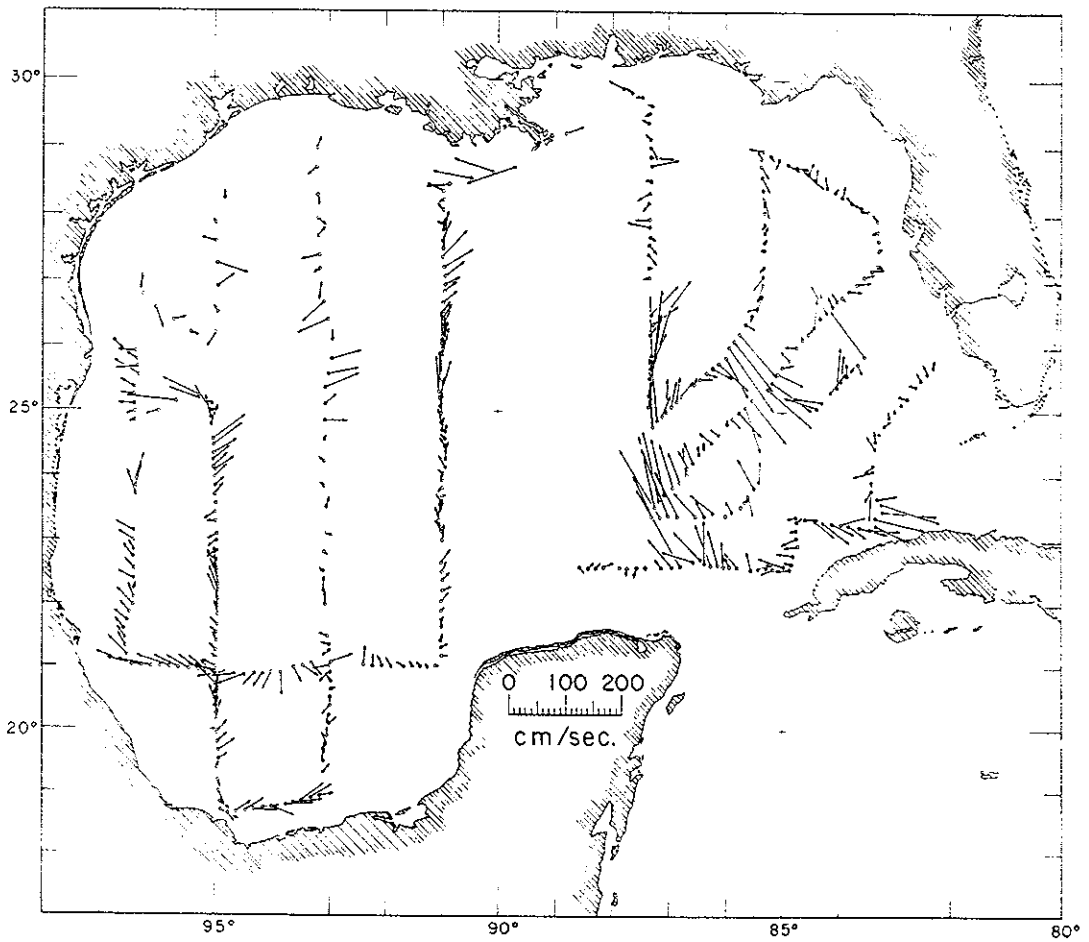

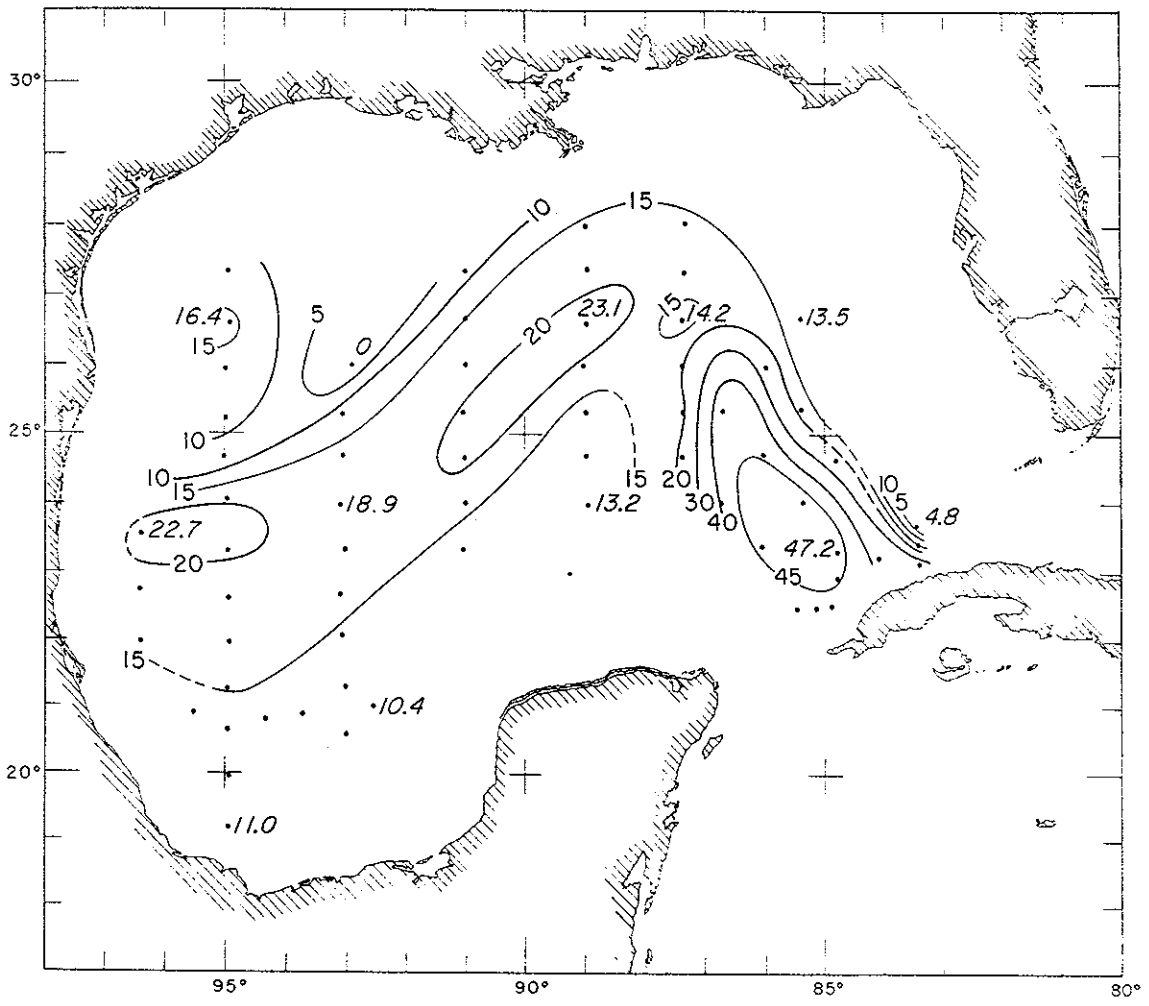

Figure 1-35. Streamlines of geostrophic transport, in 10^6 m^3*/sec, in upper 1000 db relative to the 1000-db surface,* Hidalgo *62-H-3.*

tential. Before contouring this scalar field, the minimum value of this potential function was subtracted from every value and the residual at each station was divided by the value of the Coriolis parameter at 24° latitude. Of course, the field is very similar in appearance to the dynamic topography presented in Figure 1-29.

For further discussion, the Gulf of Mexico is divided into eastern and western subregions.

Eastern Gulf

The Yucatan Current appears to turn clockwise in the eastern central Gulf and then issue into the Straits of Florida, where it is known as the Florida Current. We refer to this current in the turn-around region as the Loop Current. Based on data from any reasonably short time period, the

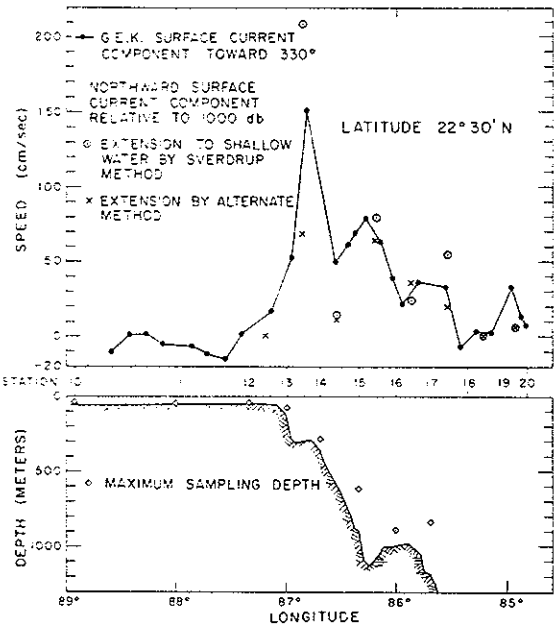

Figure 1-36a. Depth profile and surface currents along Section A *(22°30'N). Shown are GEK surface-current components toward 330° and geostrophic surface current normal to Section* A.

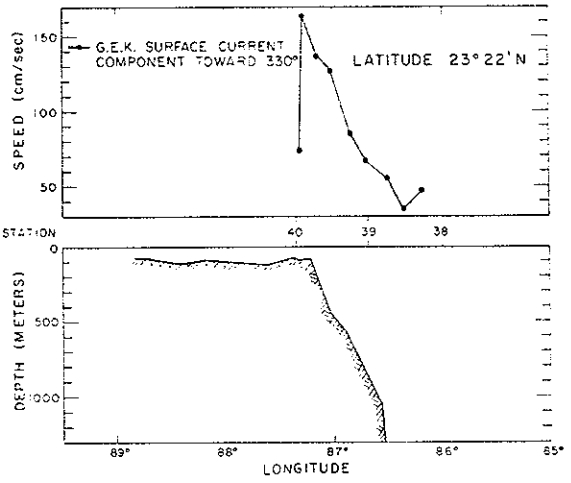

Figure 1-36b. GEK surface current components toward 330° and depth profile along a section at 23°22'N. All data from both sections collected during Hidalgo *62-H-3. For positions of stations, see Figure 1.1.*

configuration of this loop is easily defined by dynamic computations, by salinity values at the salinity maxima, and/or by the characteristic *T-S* relationship of all stations on the Cuban side of the main current.

Cochrane (1963) presented GEK data which indicate that the Yucatan Current in the region of the Yucatan Strait is kinematically banded, showing two or more high-velocity cores. This feature shows in the GEK surface-current profile across Section *A* (Figure 1-36*a*). It is not seen in the profile taken along 23°22'N, which is presented in Figure 1-36*b*. This is not inconsistent with the results of Cochrane, which show a weakening of this intercore shear zone in the downstream direction. Surface velocity components in the direction 330° are shown, since this was judged to be the orientation of the current axis during the period of observation. This banding is also evident in the temperature profile (Figure 1-20) along Section *A*. Referring to the GEK surface velocities for Section *A* in Figure 1-34, it is seen that in the Yucatan Current between the two apparent high-velocity cores there is a considerable component of velocity directed toward the Yucatan Shelf.

The waters at the positions of the two cores in the current are different. At St. 13 and in the high-velocity core just west of St. 14, water of the type that characterizes the eastern Yucatan Shelf (Figure 1-4) was found. At St. 15, within the secondary current core, the waters showed the salinity maximum and smooth *T-S* relationship characteristic of the waters bounded by the Loop Current.

At Section *A*, the main core, with axial velocity components of approximately 150 cm/sec, was situated approximately over the 300-m isobath (Figure 1-36*a*). Cochrane (1965) found a sharp core situated approximately over the 200-m isobath when the surface currents were the strong-

est (average maximum velocity component of 177 cm/sec), during late spring and early summer. A more diffuse core lies farther offshore in late fall when the current reaches its minimum (average maximum axial-velocity component of 127 cm/sec).

In the downstream profile taken along 23°22'N (Figure 1-36*b*) there was only one high-velocity core (160 cm/sec). This was situated approximately over the 100-m isobath at the edge of the Yucatan Shelf.

Also presented in Figure 1-36 are components of geostrophic surface velocities normal to Section *A*. These have been computed from geopotential anomalies relative to 1000 db for adjacent station pairs. Since the maximum sampling depths for stations west of St. 18 were less than 1000 m, the section was extended into shallow water, using the method of Sverdrup et al. (1942: 451). A simpler method of extending the section was tried and is presented for comparison. In the alternate analysis, the geopotential anomaly of the sea surface relative to the maximum pressure sampled was computed. To this was added the geopotential anomaly (relative to 1000 db) at that same pressure surface for the deeper adjacent station to the east. Perhaps fortuitously, the banded nature of the surface velocity field also appears in these geostrophic computations.

Downstream from the two sections shown in Figure 1-36, the maximum current speeds indicated by the GEK ranged from 100-200 cm/sec. The largest values were observed approximately 160 nautical miles (300 km) north of Section *A*, near St. 56.

Recent results of Schmitz and Richardson (1968) based on the average of three years of direct measurements of transport by free instrument technique give 32± 3 x $10^6 m^3$/sec as the mean volume transport of the Florida Current east of Miami. They estimate that the component of this flow derived from the Santaren Channel, and not from the Straits south of the Florida Keys, is only 1-3 x 10^6 m^3/sec. Schmitz and Richardson observed a fluctuation bound of ± 12 x $10^6 m^3$/sec, of which about 75% occurs at frequencies near 1 cycle per day. The principal tidal transport fluctuations were delineated by harmonic analysis; the transport amplitudes obtained were 1.5 ± 1 x $10^6 m^3$/sec for S_2 and 3.5 ± 1 x $10^6 m^3$/sec for each of M_2, O_1 and K_1 components. They found no evidence for net transport fluctuations larger than 3 x $10^6 m^3$/sec at nontidal, e.g., seasonal, periods.

Between Sts. 24 and 26 in Section *C*, the 1962 data give an eastward volume transport relative to 1000 db (Figure 1-35) of 30.0 x $10^6 m^3$/sec. (The transport values given in the text were computed with the Coriolis parameter corresponding to the average latitude of stations considered.) The agreement between this transport value and the mean transport reported by Schmitz and Richardson is remarkable. This flow is greatly intensified southward, with maximum surface velocities being found near St. 25, as seen in the GEK observations or in the temperature and salinity distributions for Section *C* (Figure 1-23). Much of the outflow must consist of waters that are characteristic of the interior Gulf rather than of the Caribbean, since waters with a salinity maximum typical of the northwest Caribbean were found only at St. 24. In the northern part of Section *C* the data evidence some flow to the west. Relative to 500 db, the westward inflow in the upper 500 m between Sts. 26 and 28 was just over one million m^3/sec—not large when compared with the outflow.

It should not be inferred that the stream is typically found near the Cuban coast. In fact, north-south spatial fluctuations of the edges and axis of the stream are known to be pronounced in the region south of the Florida Keys. Based on GEK transects south of Key West, Hela et al. (1954) have shown the current to sometimes occupy the northernmost part of the strait, sometimes the southernmost part.

No good estimate of inflow can be prepared from the 1962 data across Section *A*. However, based on the outflow at Section *C*, continuity demands that the net inflow in the upper 1000 m across Section *A* must be some 30 x $10^6 m^3$/sec. The gross inflow in the Yucatan Current must be

even larger, since, relative to 1000 m, somewhat over one million m^3/sec is transported southward over Section *A* between Sts. 18 and 20. Most of this southward transport takes place at depths greater than 500 m.

Apparently, about 10 x $10^6 m^3$/sec of this inflow branches westward from the Yucatan Current in the region of the northern Campeche Bank. The transport in the upper 1000 m of the Loop Current is approximately 24 x $10^6 m^3$/sec between Sts. 55 and 57. Along its northeastern portion the transport in the Loop Current increases in a downstream direction as additional waters from outside the Loop join the flow.

In addition to the Loop Current proper, during the winter of 1962 some 5 to 10 x $10^6 m^3$/sec of water having characteristics typical of the northwestern Caribbean were circulating as an anticyclonic gyre within the Loop.

Although it is believed that the description of the eastern Gulf just presented is a fair picture of the circulation as it existed during the winter of 1962, this should/not be accepted as a typical picture. Recent studies have shown without doubt that the current patterns of that region are quite time dependent. The temporal variations seem especially strong from late spring until mid-fall. Perhaps this is because the Yucatan Current begins its intensification in spring, reaching maximum speeds in May (Cochrane, 1966), and according to the pilot charts it is fall before this current reaches its minimum intensification, with a relatively broad core of lesser maximum speeds.

At times the Loop Current extends much further into the northeast Gulf than was observed in the winter of 1962. As an example, in the first thorough study of the Loop Current, which was based on *Alaminos* 66-A-8 data collected during June, 1966, Hubertz (1967) found the current core at the northernmost limit of the Loop to be between 27° and 28°N, just offshore from the 2000-m depth contour along the continential slope (see Chapter 6). At other times the Yucatan Current enters the Gulf of Mexico on a northeastward course and proceeds just north of the coast of Cuba toward the Straits of Florida. In these cases, e.g., the data from *Alaminos* 65-A-12 in September, 1965 (Cochrane, 1966), there may be no extension of the Loop Current into the Gulf, only a continuation of the Yucatan Current directly toward the Straits of Florida.

There have been several occasions on which anticyclonic rings of current were observed distinct from, and outside of, the Loop Current regime. The first of these to be observed in detail and reported in the literature (Nowlin et al., 1968), was studied on *Alaminos* 67-A-4 during June, 1967. Figure 1-37, taken from Nowlin et al. (1968: figure 1), shows the depth of the 22°C isothermal surface as inferred from bathythermograph observations and also shows surface GEK measurements (corrected only for magnetic field intensity). The shear in the zone separating the ring from the Loop Current is seen to be extremely strong. The data show that both within the ring and southeast of the Loop Current the salinity values at the core of the subtropical salinity maximum were in excess of 36.7 per mil, although maximum salinity values along the axis of the shear zone separating the ring and the Loop Current were less than 36.5 per mil. (That this difference is sufficient to delineate waters bounded by the Loop Current from the other waters of the Gulf is readily seen in Figure 1-17*a*.) On *Alaminos* Cruise 69-A-7 during May, 1969, Cochrane (1969, personal communication) first observed conditions just as a ring was in the stage of separating from the Loop Current and then later surveyed much of the separated anticyclonic current ring.

Based on circulation patterns inferred from contours of isotherm depths obtained from BTs on a sequence of cruises within the time period July, 1965, to November, 1966, Leipper (1970) concluded "that there may be a systematic development and breakdown of the pattern of the Loop Current in the Gulf of Mexico," and that "this development may have some seasonal aspects." It is well established through the unpublished work of Cochrane (cited in this chapter) that there are some seasonal aspects to the development of the eastern Gulf circulation. Cochrane has docu-

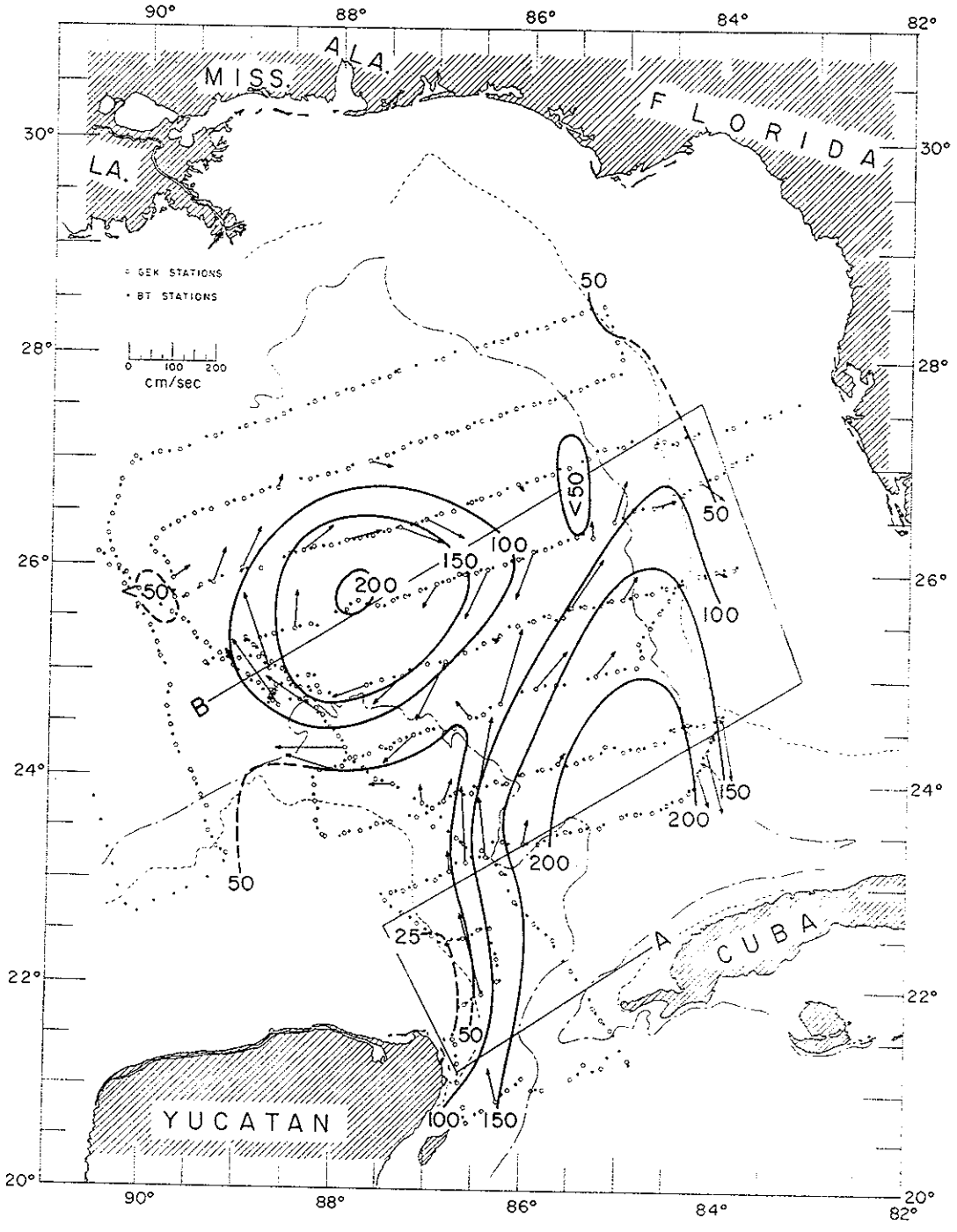

Figure 1-37. Depth (50-m intervals) of the 22°C isothermal surface from BT observations, and selected GEK surface-current measurements; Alaminos *67-A-4, June, 1967.*

mented the characteristics of the Yucatan Current during its period of development to maximum intensity in spring and has likewise established its characteristics in fall during least intensification.

Since the circulation, in the eastern Gulf at least, is driven principally by the Yucatan Current, it is reasonable to expect some seasonal aspects, although a regular seasonal pattern seems unlikely. Very complete pictures in successive seasons, e.g., in June of 1966 and of 1967, have given radically different eastern Gulf circulations: a strong Loop Current extending far into the Gulf in 1966; a large anticyclonic ring detached from the Loop Current in 1967 (see Chapter 6). It seems likely that the specific circulation patterns which develop, while having seasonal aspects derived from the driving forces, will depend strongly on local dynamics and may well not be entirely deterministic.

The faculty and students of Texas A&M University's Department of Oceanography are continuing a series of theoretical investigations of the effects on the eastern Gulf circulation of friction, of topographic control, of stratification and of the westward intensification, total transport and inflow angle of Yucatan Current. Preliminary numerical and analytical studies of the effects of lateral and vertical friction without bottom topography are complete (Wert, 1968 [see Chapter 8] Jacobs and Nowlin, 1968). Molinari (1968) studied the effects of topography of that portion of the Yucatan Current along the east and northeast edge of the Campeche Bank during the time of the year when the current is most intense; data from May, 1962, 1965 and 1966 were compared with calculated results of both graphical and numerical methods for obtaining the stream path based on the conservation of potential vorticity, the actual topography and observed initial vorticity. Some of the other studies just completed or yet in progress were discussed briefly by Reid (1969).

Western Gulf

The connection between the Yucatan Current and the circulation in the western Gulf is not yet clear. From the *Hidalgo* 62-H-3 study, it seems possible that part of the Yucatan Current may leave the main stream and flow across, or along the northern edge of, the Campeche Bank to join the broad slow flow that forms the southern flank of the anticylonic ridge in the western central Gulf. (At 91°W, the computed westward transport relative to 1000 db between Sts. 71 and 73 was 9.5 x 10^6 m^3/sec.) The sampling pattern did not allow delineation of the western end of this ridge. However, a well-developed current was observed along its northern flank.

For this northern region, geostrophic current speeds at a number of levels relative to 1000 db were computed. From 24°20′N, 95°W downstream to 25°30′N, 93°W, the maximum axial components of velocity were approximately 50 cm/sec. The geostrophic speeds in the core then seemed to decrease downstream to values of some 30 cm/sec at 27°20′N, 91°W. By comparison, the GEK measurements gave a maximum speed of approximately 70 cm/sec at all three of the stream crossings made over this distance. Dynamic computations gave larger speeds at 100 m than at the surface. Along 93°W, the downstream component was almost 70 cm/sec at 100 m. Speeds decreased below 100 m but were still of the order of 20 cm/sec at 500 m. The indications are that the stream widened in a downstream direction from 95° to 91°W; apparently water was being entrained along the northern edge of this flow from a parallel counterflow located over the shelf edge.

In the southwestward counterflow, geostrophic current speeds at the surface and at 100 m were both about 30 cm/sec as measured at 93°W. Surface GEK measurements gave 50 cm/sec at this longitude and showed a current shear between these two flows of more than 100 cm/sec in a distance of 35 nautical miles (65 km).

Other available data from the western Gulf of Mexico were examined for additional north-south sections made during the winter season. In addition to *Hidalgo* 62-H-3, only three cruises appear to have data extending across the entire Gulf with sufficient sampling density that they might be useful in establishing the winter circulation pattern.

These cruises are *Hidalgo* 58-H-1, 23-30 March 1958 (McLellan 1960): *Alaminos* 64-A-2, 17-26 January 1964; and *Alaminos* 64-A-3, 27 Feburary-2 March 1964. Figure 1-38*a* shows locations of stations along north-south sections from these three cruises and from *Hidalgo* 62-H-3. Two other cruises which provided some regional coverage of the western Gulf in winter were *Mabel Taylor* 1932 and *Atlantis* 1935; the resulting sea-surface dynamic topographies relative to 1000 db are shown in Figures 1-30 and 1-31. However, sections comparable with those in Figure 1-38*a* were not made from these two cruises.

For each station in Figure 1-38*a*, the geopotential anomalies, relative to the 1000-db surface, of the sea surface and of the 500-db surface are plotted as functions of latitude in Figure 1-38*b*. Although there is clearly variation from cruise to cruise, the striking new result to be seen in this figure is the remarkable similarity between the baroclinic fields of the western Gulf in three different winters. In each case the dominant feature is a high centered about 23°40′N latitude. Moreover, there is an indication of a westward component to the north of the eastward flowing flank of this generally east-west oriented ridge.

*Figure 1-38*a. *Positions of hydrographic stations occupied on meridional sections in the western Gulf of Mexico during the winter season;* Hidalgo *58-H-1 and 62-H-3,* Alaminos *64-A-2 and 64-A-3.*

*Figure 1-38*b. *Geopotential anomalies (in dynamic m) of sea surface and 500-db surface relative to 1000 db for data from stations with positions shown.*

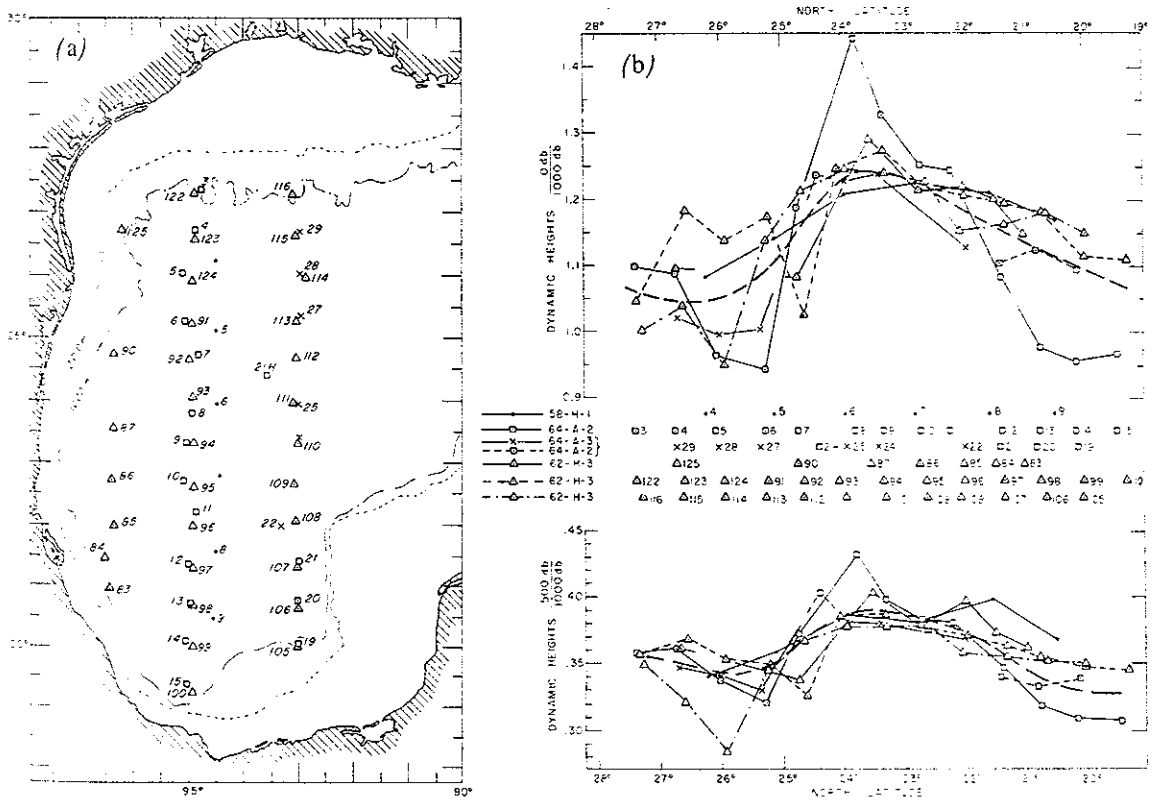

This surface pattern is generally seen also in the relative pressure field at 500 db.

Referring again to Figures 1-30 and 1-31, the results of *Mabel Taylor* and *Atlantis* 1935 are consonant with these four more recent cruises. In fact, in Figure 1-30 there is even a hint of a westward counterflow between the Texas-Louisiana Shelf and the eastward flow along the northern flank of the ridge.

In attempting to obtain a representative winter picture, as well as to quantify the variation therefrom, smooth curves were fit by eye to the geopotential anomaly data of Figure 1-38*b*. Based on data from the 61 stations shown, the standard errors were 0.067 and 0.018 dynamic meters for the relative dynamic topographies of the 0-db surface and the 500-db surface, respectively.

The available evidence points to the existence of the eastward or northeastward current as a semipermanent feature during the winter season, although its position and width are certainly variable. The westward flow over the outer shelf does not appear to be permanent; it may depend on the occurrence of low-salinity water over the outer Texas-Louisiana Shelf.

Acknowledgments

Much of the material presented here was previously presented in identical form in a series of three papers published in the *Journal of Marine Research* and authored by McLellan and Nowlin (1963), by Nowlin and McLellan (1967) and by Nowlin, Paskausky and McLellan (1969). I wish to express my appreciation to my coauthors, Drs. McLellan and Paskausky, and to the *Journal of Marine Research* for allowing me to use text and figures for these publications so freely.

All of the original work, as well as the preparation of these results, was sponsored by the Office of Naval Research through contracts with the Texas A&M Research Foundation.

My special thanks go to Mrs. Ruby Dee Parker for aid in the reduction and analyses of the data, to Mr. Oscar Chancey for preparation of the final figures and to Mesdames Ina Deel and Gwen Stevens for typing of the manuscript.

References

Austin, G. B., Jr. 1955. Some recent oceanographic surveys of the Gulf of Mexico. *Trans. Amer. Geophys. Un., 36*(5): 885-892.

Carpenter, J. H. 1965. The Chesapeake Bay Institute Technique for the Winkler dissolved oxygen method. *Limnol. Oceanogr., 10*(1):141-143.

Caruthers, J. W. 1969. T-S Characteristics of the Gulf of Mexico at intermediate depths. Unpubl. Rept. of Dept. of Oceangr., Texas A&M University, Ref. 69-7-T.

Cochrane, J. D. 1961. Investigations of the Yucatan Current. In Unpubl. Rept. of Dept. of Oceanogr. and Meteorol., The A.&M. College of Texas, Ref. 61-15F:4-7.

—— 1963. Yucatan Current. In Unpubl. Rept. of Dept. of Oceanogr. & Meteorol., The A.&M. College of Texas. Ref. 63-18A:6-11.

——.1965. The Yucatan Current and Equatorial Currents of the western Atlantic. In Unpubl. Rept. of Dept. of Oceanogr. & Meteorol., Texas A&M University, Ref. 65-17T:6-27.

——.1966. The Yucatan Current. In Unpubl. Rept. of Dept. of Oceanogr., Texas A&M University, Ref. 66-23T:14-25.

——.1967. Upwelling off northeast Yucatan. In Unpubl. Rept. of Dept. of Oceanogr., Texas A&M University, Ref. 67-11T:16-17.

——.1969. The currents and waters of the eastern Gulf of Mexico and western Caribbean. In Unpubl. Rept. of Dept. of Oceanogr., Texas A&M University, Ref. 69-9-T:29-31.

Collier, Albert, Drummond, K. H. and Austin. G. B., Jr. 1958. Gulf of Mexico physical and chemical data from *Alaska* cruises, with a note on some aspects of the physical oceanography of the Gulf of Mexico. *Spec. Sci. Rep. Fish and Wildl. Serv., Fish. 249.*

Cox, R. A. and Smith, N. D. 1959. The specific heat of sea water. *Proc. Roy. Soc., A, (London) 252*:51-62.

Defant, Albert 1961. *Physical Oceanography*, Vol. 1. London: Pergamon Press.

Duxbury, A. C. 1962. Averaged dynamic topographies of the Gulf of Mexico. *Limnol. Oceanogr.*, *7*(3): 428-431.

Franceschini, G. A. 1961. Hydrologic balance of the Gulf of Mexico. Unpubl. doctoral dissertation. The A.&M. College of Texas.

Hela, I., Chew, F. and Wagner, L. 1954. Some results of the Florida Current Survey. Unpubl. Rept., Ref. 54-7, University Miami Mar. Lab.

Helland-Hansen, Bjorn. 1930. Physical Oceanography and Meteorology. *Rep. "Sars" N. Atlant. Deep-Sea Exped., 1.*

Hesselberg, Th., and Sverdrup, H. U. 1915. Die Stabilitätsverhältnisse des Seewassers bei vertikalen Verschiebungen. *Bergens Mus Årb. (1914-1915), 15*:1-16.

Hubertz, Jon M. 1967. A study of the Loop Current in the eastern Gulf of Mexico. Unpubl. Rept. of Dept. of Oceanogr., Texas A&M University, Ref. 67-4T.

Jacobs, C. A. and Nowlin, W. D., Jr. 1968. A numerical treatment of steady, frictional boundary Currents in a homogeneous ocean applied to a two-port basin. Unpubl. Rept. of Dept. of Oceangr., Texas A&M University, Ref. 68-19T.

Leipper, D. F. 1970. A sequence of current patterns in the Gulf of Mexico. *Jour. Geophys. Res.*, 75(3):637-658.

McLellan, H. J. 1960. The waters of the Gulf of Mexico as observed in 1958 and 1959. The A.&M. College of Texas, Dept. of Oceanogr. & Meteorol., Unpubl. Rept., Ref. 60-14T.

____.and Nowlin, W.D., Jr. 1963. Some features of the deep water in the Gulf of Mexico. *J. Mar. Res., 21*(3): 233-245.

Molinari, R. L. 1968. The effects of topography on the Yucatan Current. Unpubl. Rept. of Dept. of Oceanogr., Texas A&M University, Ref. 67-24T.

Nowlin, W. D., Jr. and McLellan, H. J. 1967. A characterization of the Gulf of Mexico waters in winter. *J. Mar. Res., 25*(1): 29-59.

____, Hubertz, J. M. and Reid, R. O. 1968. A detached eddy in the Gulf of Mexico. *J. Mar. Res., 26*(2):185-6.

Paskausky, D. F. and McLellan, H. J. 1969. Recent dissolved-oxygen measurements in the Gulf of Mexico deep waters. *J. Mar. Res., 27*(1):39-44.

Parr, A. E. 1935. Report on hydrographic observations in the Gulf of Mexico and the adjacent straits made during the Yale oceanographic expedition on the *Mabel Taylor* in 1932. *Bull. Bingham Oceanogr. Coll., 5*(1).

Reid, R. O. 1969. Theoretical studies of ocean dynamics. In Unpubl. Rept. of Dept. of Oceanogr., Texas A&M University, Ref. 69-9T:52-58.

Schmitz, W. J., Jr., and Richardson, W. S. 1968. On the transport of the Florida Current. *Deep-Sea Res., 15*(6):679-93.

Sverdrup, H. U., Johnson, M. W. and Fleming, R. H. 1942. *The oceans: their physics, chemistry and general biology*. Englewood Cliffs, New Jersey: Prentice-Hall.

Wennekens, M. P. 1959. Water mass properties of the Straits of Florida and related waters. *Bull. Mar. Sci. Gulf Carib., 9*(1):1-52.

Wert, R. T. 1968. A frictional model of a two-port unbounded ocean basin. Unpubl. Rept. of Dept. of Oceanogr., Texas A&M University, Ref. 68-4T.

Wüst, Georg. 1936. Schichtung and Zirkulation des Atlantischen Ozeans. Die Stratosphäre. *Wiss. Ergebn. Dtsch. Atlant. Exped. Meteor, 6*(1) with Atlas, Berlin.

____. 1964. *Stratification and circulation in the Antillean-Caribbean basins, Pt. 1*. New York: Columbia Univ. Press.

Wilson, R. J. 1967. Amount and distribution of water masses in February and March 1962 in the Gulf of Mexico. Unpubl. M.S. Thesis, Texas A&M University.